UNCOVERseq Enables Sensitive and Controlled Gene Editing Off-Target Nomination Across CRISPR-Cas Modalities and Systems

Kyle J. Kinney[1], Kun Jia[2], He Zhang[1], Ellen Schmaljohn[1], Thomas Osborne[1], Bernice Thommandru[1], Karthik Murugan[1], Andrea Sánchez-Peña[1], Sean West[1], Shengyao Chen[1], Roshani Codipilly[1], Morgan Sturgeon[1], Rolf Turk[1], Matthew McNeill[1], Mark Behlke[1], Ashley Jacobi[1], M. Kyle Cromer[2], Garrett Rettig[1], & Gavin Kurgan[1]

[1]Integrated DNA Technologies, Coralville, IA 52241, USA

[2]Department of Surgery, University of California, San Francisco, San Francisco, CA, USA

Correspondence should be addressed to G.K. (gkurgan@idtdna.com)

Abstract

The rapid development of CRISPR-Cas gene editing technologies has revolutionized genetic medicine, offering unprecedented precision and potential for treating a wide array of genetic disorders. However, assessing the risks of unintended gene editing effects remains critical, and is complicated by new editing modalities and unclear analytical guidelines. We present UNCOVERseq (Unbiased Nomination of CRISPR Off-target Variants using Enhanced RhPCR), an improved *in cellulo* off-target nomination workflow designed to sensitively nominate off-target sites (<0.01% editing) with defined input requirements and analytical process controls to provide empirical performance evidence across diverse circumstances. Using this workflow, we nominated off-targets across 192 guide RNAs (gRNAs) and demonstrated superior performance compared to existing methodologies. We identified a subset of six gRNAs with a dynamic range of specificity and confirmed the relevance and high true positive rate of our nomination method, providing relative risk assessments for multiple modalities (*S.p.* Cas9 and derived high-fidelity variants / base editors) in a translational system involving hematopoietic stem and progenitor cells (HSPCs). Additionally, we established that double-strand break (DSB) editing retains a strong, positive rank correlation to single-strand break (SSB)-mediated base editing, highlighting the importance of DSB nomination sites as candidate loci for base editing. Overall, UNCOVERseq improves informed risk assessment of gene editing in translational systems by enhancing the quality of off-target nomination.

Introduction

CRISPR-Cas systems have revolutionized genetic engineering by enabling precise genome modifications. Derived from a bacterial adaptive immune mechanism, CRISPR-Cas9 allows targeted DNA edits in various organisms, enabling vast potential in medicine, agriculture, and biotechnology[1,2]. However, CRISPR-Cas9 faces challenges, notably off-target effects where unintended genomic regions similar to the target sequence can be edited[3,4]. This off-target activity is often due to sequence homology between the protospacer region of the gRNA and non-target regions of the genome. These off-target edits can lead to unwanted genetic changes and disrupt the function of essential genes leading to adverse effects on cellular function, viability, development of secondary diseases, or exacerbate existing conditions that pose risks in therapeutic applications.

Recent advancements in gene editing have driven the parallel development of technologies to nominate off-target editing effects[5–12]. These technologies broadly fall into three categories: cell-based *in cellulo/in situ*, computational *in silico*, and biochemical *in vitro* assays each with distinct advantages and disadvantages. Cell-based assays like GUIDE-seq are known for high precision due to their ability to accurately mimic the cellular environment[7,13,14]. While cell-based methods provide nomination in a cell-type-specific and even donor-specific manner, these methods face challenges in representing diverse genome populations and typically require biologically variable processes such as DNA double-strand breaks (DSBs) and blunt integration of a dsDNA tag through non-homologous end joining (NHEJ) as a mechanism of action. Biochemical *in vitro* assays are highly sensitive and can represent patient genotypes with diverse editing modalities since they are executed on cell-free genomic DNA, but have low precision and suffer difficulties in replicating the cellular environment, which significantly impacts enzymatic activity[6,7,13–15]. Computational *in silico* approaches can rapidly predict all candidate off-target sites with homology to the gRNA in a patient genome / population-specific manner, but result in low precision due to insufficient data to inform predicted enzymatic and biological activity across diverse cell types[11–14,16]. All methods are setback by a lack empirical data and application of standards to characterize sensitivity against known truth, as it is challenging to ascertain a complete list of true positives for each gRNA in an unbiased manner. To better standardize off-target safety assessment, comprehensive information on assessment methods and guidance for their use is essential.

55 Most methods for off-target nomination currently utilize next-generation sequencing (NGS) to detect
56 off-targets. The efficiency of library preparation, library complexity (i.e., unique genome equivalents
57 sequenced), read depth, and computational analysis methods are all known limitations affecting
58 performance of NGS methods[17]. Some work has endeavored to improve upstream biological and library
59 preparation inefficiencies of *in cellulo* methods[18,19]. Other work has presented evidence of biological
60 optimizations that proxy cell lines promiscuously editing off-targets may represent a superset of off-targets
61 in HSPCs[20]. However, exploration of other NGS variables commonly benchmarked in parallel fields to drive
62 uniformity in experimental procedures and reporting, are still largely lacking for gene editing off-target
63 nomination[17,21]. The FDA has recently worked to address this need through draft guidelines for the cell and
64 gene therapy industry, which currently recommends multiple orthogonal methods for off-target nomination[22].
65 This guideline for orthogonality ideally aims to mitigate known and unknown weaknesses in nomination,
66 including variability in NGS method execution.

67 Rapid innovations in gene editing have further complicated the off-target nomination process with
68 the discovery of various editors possessing unique qualities beyond the targeted generation of DSBs with
69 a Type II nuclease. This includes engineered systems generating staggered double-strand breaks (DSBs)
70 in Type V CRISPR-Cas systems or leveraging single-strand DNA breaks (SSBs) coupled to engineered
71 moieties for editing[23–25]. SSB engineered moieties like adenine base editors (ABE)[26], cytosine base editors
72 (CBE)[27], and prime editors (PE)[28] offer benefits such as decreased frequencies of unintended indels and
73 even the ability to make non-indel DNA changes typically reserved for homology-directed repair (HDR).
74 However, they lack consensus guidance regarding appropriate nomination assays for off-target
75 assessment, and previous work has largely used DSB nomination methods as a proxy[29,30]. Due to the
76 nature of these editors to generate both indels and SNPs, an orthogonal approach specializing on each
77 event type may be needed to sensitively nominate off-targets.

78 In this work, we develop an optimized end-to-end *in cellulo* nomination method and analysis
79 pipeline, UNCOVERseq (Unbiased Nomination of CRISPR Off-target Variants using Enhanced RhPCR),
80 leveraging NHEJ-based dsDNA tag integration for RNase H-dependent PCR (rhPCR)-based library
81 preparation[31]. We demonstrate that using this method with a cell line under promiscuous editing conditions
82 serves as a sensitive proxy for clinically relevant cell types. We establish experimental recommendations

83 for library complexity, coverage depth, and end-to-end process controls that reliably lead to the successful
84 nomination of risk-tiered edited sites with sub-0.01% editing (indel) frequencies observable empirically. By
85 screening 192 gRNAs using UNCOVERseq, we identify an experimental set of gRNAs spanning a broad
86 range of specificities that are broadly representative of use-cases encountered in the field. We find that off-
87 target effects of base editors are directly, rank-order correlated to DSB editing frequencies, demonstrating
88 UNCOVERseq as an effective technology for nominating meaningful off-targets for both current and next-
89 generation editing modalities. We conclude that, regardless of editor modality, the off-target burden of
90 gRNAs quickly decreases to frequencies not measurable – that is, below the limit of detection - with current
91 NGS methods (0.01% for indels and 0.5% for base editing) as gRNA specificity scores rise. However, off-
92 targets may still be observable at higher specificities in an editor/gRNA-dependent manner, emphasizing
93 the need to consistently and empirically nominate and interrogate off-targets across the specificity
94 spectrum.

95 **Results**

96 **Development and optimization of UNCOVERseq**

97 To create our nomination method, we first started with the original GUIDE-seq protocol and
98 designed a novel orthogonal dsDNA sequence with sufficient length to perform a modified rhPCR to
99 multiplex primers in close proximity within a single reaction while avoiding primer-dimers (Supplementary
100 Table 1). To streamline the process for preparing the nomination gDNA libraries we additionally converted
101 from a mechanical to enzymatic fragmentation (Figure 1A). Upon analyzing data, we observed that freely
102 adaptered dsDNA tag was allocated an average range of 37% to 67% of reads, varying across 4 gRNAs
103 (Figure 1B). This same artifact was also observed with the original GUIDE-seq protocol (Supplementary
104 Figure 1). To improve usable reads resulting from NGS, we introduced a blocking oligo into the PCR1
105 preparation designed to target the adapter:dsDNA junction (Figure 1A). Introduction of this blocker reduced
106 reads belonging to the adapter:dsDNA artifact to an average range of 0.3% to 0.5%, meaning >99% of
107 reads were now belonging to gDNA:dsDNA junctions (Figure 1B). Nomination frequencies were found to
108 be conserved for all gRNAs (R^2=0.99) with and without the blocking oligo (Supplementary Figure 2).

109 In parallel to creation of the wet-lab protocol, we created an analysis pipeline with features such as
110 heuristic nomination criteria (Levenshtein distance < 7; read-evidence from both sides of a prospective off-
111 target), statistical comparison of treatment:control samples as nomination criteria (FDR < 0.05) and
112 integrated genomic annotations. We then investigated optimizations in the computational pipeline for
113 nomination of gRNAs using a set of 48 gRNAs spread across the *PDCD1*, *LAG3*, *CTLA4*, *NRP1*, *IL2RA*,
114 and *TIGIT* genes. In off-target nomination, off-target loci are generally determined to be trustworthy based
115 on: 1) frequency, 2) reproducibility, and/or 3) similarity to the intended target sequence (gRNA), with
116 Levenshtein distance > 6 often being used to disqualify an off-target.

117 To investigate the effect of alignment method used for determination of an off-target list, we tested
118 existing GUIDE-seq pipeline methods (https://github.com/aryeelab/guideseq; commit: 997b892; fuzzy
119 regular expression based; Regex) and historical GUIDE-seq pipeline methods
120 (https://github.com/aryeelab/guideseq; tag:v1.0; Smith-Waterman alignment with -100/-100 gap
121 open/extension penalty) as compared to a glocal implementation of the Needleman-Wunsch algorithm.
122 Investigation of 48 different gRNAs found a significant difference in the number of Levenshtein distance <
123 7 loci nominated using each approach, and that the glocal Needleman-Wunsch alignment approach yielded
124 a median of 30% and 150% more qualified off-target locations than the current and historical GUIDE-seq
125 analysis approaches (Figure 1C). To do an end-to-end comparison of the current GUIDE-seq method to our
126 method, we did a complete workflow comparison across the same 48 gRNAs and found that our method
127 nominated a range of 60% to 4,150% more off-targets per gRNA, with an average of 132 off-targets as
128 compared to 23 using the GUIDE-seq protocol (Figure 1D). We termed the final instantiation of the end-to-
129 end method as UNCOVERseq (Unbiased Nomination of CRISPR Off-target Variants using Enhanced
130 RhPCR; v1.0).

131 **Promiscuous cell systems as sensitive UNCOVERseq proxy nomination models**

132 To identify ideal biological operating conditions, we explored biological variables with potential
133 workflow impacts on nomination performance. Promiscuous editing conditions are known to increase
134 editing frequencies at off-targets, which we hypothesize should increase the sensitivity of *in cellulo* methods
135 like UNCOVERseq (Figure 2A). To test this, we selected 4 – 10 gRNAs per cell line and nominated off-

136 targets using UNCOVERseq in K562, iPSCs (wildtype *S.p.* Cas9 or HiFi Cas9), primary T-cells, or a
137 promiscuous HEK293 cell line stably expressing *S.p.* Cas9 (HEK293-Cas9). Investigation of the overlap of
138 off-target frequencies between these cell lines and HEK293-Cas9 found an average of 99.7% to 100% of
139 total UMI-corrected events (corresponding to total frequency) in each cell line could be found in the off-
140 targets of just a single replicate of HEK293-Cas9 (Figure 2B). Comparison of shared nomination
141 frequencies showed a high rank-order correlation for HEK293-Cas9 nominated off-targets between K562
142 (r = 0.63), iPSC (r = 0.61), and primary T-cells (r = 0.69), demonstrating that the frequency-based
143 importance of different off-targets for prioritization was still largely conserved (Figure 2C-E). We also
144 observed that the overall nominated off-targets number for the same gRNAs could vary significantly in
145 different primary cell lines for the same gRNAs, with low numbers of off-targets nominated in iPSCs, further
146 demonstrating why a promiscuous system can be used to remove this variable (Figure 2F). Overall
147 nomination in a promiscuous cell line like HEK293-Cas9 was capable of generating an average of 196% to
148 1,560% more candidate targets per gRNA compared to an efficient primary cell type for nomination, like
149 primary T-cells, supporting that this is a more sensitive model for off-target nomination even in translational
150 contexts (Figure 2G).

151 **Off-target reproducibility using UNCOVERseq**

152 To assess sample-to-sample reproducibility, we compared biological triplicates of UNCOVERseq
153 in HEK293-Cas9 across four gRNAs. An average of 99.2% to 99.7% of instances based on frequency were
154 shared between any two biological replicates, indicating high frequency sites are consistently captured with
155 a single replicate (Figure 3A). Frequency rank order of off-targets was highly conserved (R^2=0.997) across
156 replicates as well (Figure 3B). This indicates that both frequencies and sites containing the majority of reads
157 are highly reproducible between UNCOVERseq replicates.

158 To determine ideal experimental conditions for off-target nomination, we characterized factors
159 affecting reproducibility in a functional context. When making decisions about nominated off-targets, ideally
160 off-targets are prioritized based on: a) frequency, b) reproducibility, and c) genomic impact. To this end, we
161 developed a tiering system based on UNCOVERseq data to prioritize off-targets for confirmation (Tier 1 to
162 3) from less important ones (Supplementary Table 2). To assess reproducibility for prioritizing important off-

163 targets (Tier 1-3), we compared biological triplicates to single replicates of the previous 48 gRNAs in
164 HEK293-Cas9. Without biological triplicates, 30% to 40% of high priority off-targets were not captured or
165 prioritized (Figure 3C). The average frequency of missed high priority targets increased with gRNA
166 specificity, though this is partially because the denominator (total off-targets) is smaller (Figure 2C). While
167 high frequency events were reproducible (Figure 3A), low frequency events lacking full reproducibility or
168 those in important genomic contexts (e.g., exonic) were not appropriately identified without replicates
169 (Figure 3C).

170 Replication additionally theoretically allows more appropriate tiering of off-targets. To investigate
171 the effect of tiering on the downstream requirements for confirmation, we compared the number of off-
172 targets nominated for appropriately tiered off-targets of biological triplicates (Tier 1 to 3) versus all off-targets
173 of a single replicate. We observe that even though replicates lead to more off-targets nominated, the
174 number of off-targets for interrogation are roughly equivalent when using tiering criteria (Figure 3D). This
175 provides evidence that tiering off-targets in replicate nominations leads to more impactful sites being
176 nominated and recommended for interrogation without significantly increasing the number of off-targets
177 recommended.

178 **Determination of UNCOVERseq sensitivity and process controls**

179 To characterize the sensitivity of UNCOVERseq and create routine process controls, we extensively
180 characterized the off-targets of a promiscuous gRNA for use as a positive control. Using a promiscuous
181 *LAG3*-targeting gRNA (*LAG3* site 9), we nominated off-targets in 12 biological replicates using HEK293-
182 Cas9. All replicates showed high editing (>90%) with tag integration frequencies between 64% and 81%
183 (Figure 4A). A total of 2269 unique nominated sites were identified, with 723 consistently reproduced across
184 all replicates (Figure 4B). The relative rate at which off-targets could not be reproduced between each
185 subsequent replicate rapidly dropped below <5% after 3 replicates and decreased linearly afterwards
186 (Figure 4B). Although only off-targets reproduced in all replicates were chosen for downstream confirmation,
187 this suggests that after three replicates real off-targets that were harder to reproduce due to low frequencies
188 and random sampling differences may be lost from high replication requirements.

189 To subset off-targets into different groups, we developed five Severity Bins based on the nomination
190 frequency of the off-target relative to the identified on-target event (Supplementary Table 3). These were as
191 follows: Severity Bin 1, >50%; Severity Bin 2, 10 - 50%; Severity Bin 3, 1 - 10%; Severity Bin 4, 0.5 – 1%;
192 Severity Bin 5, <0.5%. To monitor editing frequencies, we selected 12 sites from each frequency bin
193 (Severity Bin), creating a subset of 60 sites for sequencing and confirmation (Figure 4C; Supplementary
194 Figure 3; Supplementary Table 6). Confirmation of editing for these sites in HEK293-Cas9 showed
195 significant indels ranging from 88% to 0.02%, approaching our sensitivity limit (0.01%) (Figure 4D; Figure
196 4F).

197 Of the interrogated panel, 100% of sites in Severity Bin 1 to Severity Bin 3 had confirmed editing
198 (Figure 4D). 72.3% of sites in the <0.5% nomination frequency bin (Severity Bin 5) and 30% in the 0.5 to
199 1% nomination frequency bin (Severity Bin 4) could not be confirmed down to 0.01% indels (Figure 4D).
200 This linear decrease suggests that UNCOVERseq nominates sites with frequencies below 0.01% indels
201 (Figure 4D). This may be due in part to the higher genomic DNA input in UNCOVERseq (500 ng) as
202 compared to the subsequent confirmation library preparation (100 ng). In high specificity conditions (SpyFi
203 Cas9 + ribonucleoprotein nucleofection), fewer off-targets were edited, but a similar dynamic range of
204 confirmed editing was retained (0.03% to 85% indels), with 100% of sites with confirmed editing
205 successfully nominated (Figure 4E). This indicates the approach can be used as a process control to ensure
206 high sensitivity with reportable metrics. UNCOVERseq nomination frequencies were highly correlated
207 (R^2=0.74) with confirmation frequencies (Figure 4F). The high true positive rate and consistent decrease in
208 confirmation success in bins approaching our detection limit suggest these sites represent ~100% true
209 positives.

210 **Determination of UNCOVERseq input and sequencing requirements**

211 The number of genomes in an amplification reaction and the number of sequencing reads allocated
212 are key limiters for NGS assay performance. To maximize sensitivity, all UNCOVERseq experiments used
213 ~150,000 genome equivalents. While gDNA input could potentially be increased, we rationalize that this
214 amount of gDNA is attainable by most experimental conditions and represents the ability to potentially

215 detect down to 0.001%, which is below the limit of detection for any currently published confirmation
216 techniques for CRISPR gene editing.

217 To characterize read depth requirements for reproducible off-target nomination, total reads were
218 downsampled from the previous *LAG3* site 9 UNCOVERseq dataset (n = 12) to frequencies ranging from
219 3 million to 10,000 reads per sample. Prior to downsampling, editing across confirmable sites showed
220 interquartile range (IQR) frequencies for each Severity Bin as follows: Severity Bin 1, 26%-48%; Severity
221 Bin 2, 2.6%-7.6%; Severity Bin 3, 0.13%-0.82%; Severity Bin 4, 0.06%-0.13%; and Severity Bin 5, 0.01%-
222 0.02% (Figure 4G). Thus, this dataset represents the full dynamic range of what can currently be detected
223 by confirmation (>0.01% indels). High frequency sites in Severity Bin 1 and Severity Bin 2 were nominated
224 with 100% sensitivity using 50,000 reads per sample (Figure 4H). To nominate down to 0.01%-0.02% indel
225 frequencies with 100% sensitivity, at least 2 million reads per sample were required (Figure 4H). Given the
226 tendency of HEK293-Cas9 cells to over-nominate off-targets, we recommend performing UNCOVERseq
227 with >500,000 reads per sample to aim for >50% analytical sensitivity at Severity Bin 5, and >2 million reads
228 per sample for maximum sensitivity in assessing candidate off-target sites (Figure 4H). It is possible that
229 read depth requirements may vary with off-target number. However, by using a promiscuous gRNA
230 (specificity score = 0.013) to determine this value, we propose that this represents the number of reads to
231 successfully nominate sites even with gRNAs with very poor specificity.

232 **Comparative analysis of UNCOVERseq to other nomination methods**

233 A comparative analysis of UNCOVERseq to peer-reviewed accounts of other nominations methods
234 was performed to better understand how the sensitivity and nomination frequencies of diverse methods
235 compare. Due to variable operational conditions, precision, and total nomination list sizes reported of
236 different methods, we postulate that sensitivity is most appropriately measured using either off-targets with
237 confirmed editing or off-targets from methods with high precision. Interrogation of the 60 *LAG3* site 9 gRNA
238 off-targets compared to CHANGE-seq[7] and GUIDE-seq[7] nominations demonstrated that both methods
239 could nominate the most frequent group of confirmed off-targets (Severity Bin 1) with 91% - 100%
240 sensitivity, but sensitivity rapidly decreased in the lower frequency off-target bins. CHANGE-seq was
241 demonstrated to have a sensitivity between 66% to 75% for recovering Severity Bin 3 to 5 off-targets, while

242 GUIDE-seq had a linear decrease from 16% to 0% for these same Severity Bins of confirmable off-targets
243 (Supplementary Figure 4).

244 Random sampling of the *LAG3* site 9 dataset with 100% reproducibility showed UNCOVERseq-
245 nominated sites had ~100% precision, with confirmation frequencies correlating to average nomination
246 frequencies (Figure 4). Using this logic, we postulate the full 723 sites in this fully reproducible set are also
247 likely to represent true positives. Investigation of sensitivity and frequencies of previous accounts of
248 CHANGE-seq and GUIDE-seq for this gRNA yielded similar trends in sensitivity per Severity Bin, further
249 supporting this (Figure 5A). This provides additional evidence that reproducible UNCOVERseq sites have
250 high likelihood of being true positives and may serve as an appropriate proxy for measuring sensitivity of
251 different methods.

252 Using our previous finding that off-targets with >3 replicates reproducing a site is likely indicative of
253 true positives (Figure 4B), we compared fully reproduced off-targets from 6 biological replicate
254 UNCOVERseq experiments for three gRNAs (*EMX1*, *FANCF*, and *PCSK9*) to previous accounts of off-
255 targets from GUIDE-seq[5], INDUCE-seq[10], Olitag-seq[18], CHANGE-seq[7], CIRCLE-seq[6], AID-seq[32], BLISS[33],
256 ONE-seq[34], DIG-seq[35], Digenome-seq[34], and SITE-seq[8] nomination methods (Supplementary Table 5). For
257 PCSK9, only a combined set of ONE-seq and Digenome-seq sites was available, and nomination sensitivity
258 was found to fluctuate from 0% to 83% through Severity Bins 2 to 5 (Figure 5B). For *EMX1*, DIG-seq and
259 BLISS sensitivity decreased to 29% and 57% after Severity Bin 1, respectively, and sharply decreased at
260 lower frequency bins. Cell-based methods GUIDE-seq, Olitag-seq and INDUCE-seq sensitivity dropped
261 after Bin 2 (11% to 53% sensitivity), ranging from 55% to 0% for off-target nomination frequencies observed
262 after Severity Bin 2 (Figure 5C). However, nomination frequencies for GUIDE-seq, Olitag-seq and INDUCE-
263 seq correlated well with expected frequencies (R^2 = 0.52 to 0.70), if identified (Supplementary Figure 5).
264 Remaining biochemical *in vitro* nomination methods had the highest sensitivity compared to UNCOVERseq,
265 with approximate rank-order as follows: AID-seq/SITE-seq > CHANGE-seq > CIRCLE-seq (Figure 5C).
266 Sensitivity dropped for all these methods at Severity Bin 3, and ranged from 37% to 95% for Severity Bin 3
267 to 5 (Figure 5C). For *FANCF*, GUIDE-seq and DIG-seq sensitivity quickly decreased below 50% after
268 Severity Bin 2 to a range from 0% to 21% below Severity Bin 3 (Figure 5D). AID-seq/SITE-seq achieved

269 higher sensitivity compared to CIRCLE-seq/CHANGE-seq, similar to previous observations with EMX1
270 (Figure 5C-D). CHANGE-seq and CIRCLE-seq sensitivity dropped to a range of 67% to 78% after Severity
271 Bin 1 (Figure 5D). SITE-seq and AID-seq sensitivity dropped after Severity Bin 2 and ranged from 75% to
272 100% (Figure 5D).

273 In this calculation of sensitivity per method, each method nominated a widely variable number of
274 sites per gRNA, which affects this calculation. The number of nominated sites ranged from 9 for *FANCF*
275 using GUIDE-seq to 6,849 off-targets using *LAG3* site 9 with CHANGE-seq (Figure 5E). While biochemical
276 *in vitro* methods like CHANGE-seq, AID-seq, and SITE-seq showed the greatest comparative sensitivity,
277 they also had the largest nominated site list, ranging from 291 to 1,328 sites for the *FANCF* and *EMX1*
278 gRNAs shared between most methods (Figure 5E). Investigation of method normalized nomination
279 frequencies demonstrate that *in vitro* methods have the poorest correlation to UNCOVERseq derived
280 frqeuencies (R^2 = 0.01 to 0.26), with AID-seq and SITE-seq having the lowest correlations (Supplementary
281 Figure 5). Nomination frequencies derived from cell-based *in cellulo* and *in situ* methods (GUIDE-seq,
282 OliTag-seq, INDUCE-seq, BLISS) better correlate to UNCOVERseq nomination frequencies (R^2 = 0.31 to
283 0.70), which previously were shown to correlate to observed confirmation frequencies (Supplementary
284 Figure 5; Figure 4F; Figure 5). These findings demonstrate that UNCOVERseq improves upon the
285 sensitivity of existing *in cellulo* methods such as GUIDE-seq, in addition to subsequent improved
286 methodologies such as OliTag-seq. Our findings also demonstrate that *in vitro* methods are not inherently
287 more sensitive than *in cellulo* methods for discovering true off-targets, and UNCOVERseq nominates
288 confirmable off-targets not detected in other methods.

289 **Screening gRNAs of variable specificity**

290 To identify the specificity of a broad set of gRNAs for future experimental design, 192 gRNAs were
291 selected and UNCOVERseq performed in HEK293-Cas9 cells. Samples were sequenced to a median of
292 1.8 million reads, in line with our previous recommendations for maximizing sensitivity (Supplementary
293 Figure 6A). Following this, we calculated a specificity score for each gRNA as previously defined[7]. We
294 rationalized that only a single replicate per gRNA was needed for this experimentation since we were most
295 interested in higher frequency off-targets that would be recovered from a single replicate in the promiscuous

296 system (Figure 3A). A range of specificity scores per gRNA were recovered ranging from 0.00063 to 1.0
297 (Supplementary Figure 6B). Comparison to previously published CHANGE-seq specificity scores of
298 overlapping gRNAs demonstrated a high rank-order correlation (r = 0.63) between specificity scores derived
299 from both methods, though sometimes large disagreements in specificity scores for higher specificity
300 gRNAs occurred (Supplementary Figure 6C). We then subset gRNAs by specificity scores (binned in
301 increments of 0.2) and obtained a relatively uniform distribution with each bin containing a range between
302 22 to 47 gRNAs each (Supplementary Figure 6D-E). We further subset these gRNAs by those that were
303 ABE- and CBE-compatible as defined as having either an "A" in the +4 to +7 positions (5' to 3') or a "C" in
304 the +4 to +8 positions (5' to 3'). This resulted in a less uniform distribution of gRNAs across the specificity
305 spectrum with a range of 8 to 21 gRNAs per specificity score bin (Supplementary Figure 3D-E). From this
306 we selected six gRNAs for further experimentation as representing a continuous range from 0 to 1
307 supporting all editor modalities: *PDCD1* site 8, *CYP2C18*, *RNF2*, *TRAC* site 7, *B2M* site 1 and *TIGIT* site 7
308 (Figure 6A).

309 **Comparative analysis of editors in HEK293-Cas9 and HSPCs (on-target)**

310 Next, we sought to determine the translation of UNCOVERseq off-targets across a broad range of
311 specificities in a translational ex-vivo system (HSPCs with mRNA editor nucleofection) across different
312 editing modalities (DSB Cas9, SSB Base Editors, SSB Prime Editors). To do this, we edited HSPCs with
313 one of six gRNAs along with mRNA of either a) a high fidelity *S.p.* Cas9,variant (HiFi Cas9) b) *S.p.* Cas9
314 (D10A) fused to a Cytosine Base Editor (AncBE4max[36]), c) *S.p.* Cas9 (D10A) fused to Adenine Base Editor
315 (ABE8e[37]) and d), *S.p.* Cas9 (H840A) fused to the PE2 system[28] with a pegRNA intended to introduce a
316 single SNP. HEK293-Cas9 was also edited in parallel with the wildtype *S.p.* Cas9 nuclease. Evaluation of
317 on-target *S.p.* Cas9 editing found that editing in HEK293-Cas9 was highly efficient at all sites, ranging from
318 60.4% to 99.4% indel editing, but with a trend of decreased frequencies at lower specificity gRNAs (Figure
319 6B). Evaluation of on-target indel editing in HSPCs had a range of 4.4% to 88.4% indel editing for the DSB-
320 based HiFi Cas9 editor, 0.0% to 2.3% indel editing for ABE editors, and 0.0% to 3.8% indel editing for CBE
321 editors, and 0.0% to 0.36% indel editing for Prime Editors (Figure 6C). Intended on-target cumulative base
322 editing ranged from 16.5% to 75.9% for ABEs, and from 0.78% to 32.9% for CBEs (Figure 6D). No

323 significant base editing was observed for either the DSB-based *S.p.* Cas9 editors or SSB prime editor, as
324 would be expected (Data not shown). No significant frequencies were observed for the intended mutation
325 to be introduced via prime editing at any sites (Data not shown). For this reason, we excluded further
326 evaluation of the prime editor. Since we show evidence of on-target indel editing with the PE construct, we
327 hypothesize the lack of intended activity is due to the need for substantial pegRNA optimization to achieve
328 successful prime editing, as has been previously reported[38]. For all editors in HSPCs, similar trends were
329 observed to HEK293-Cas9 that the lower specificity gRNAs *PDCD1* site 8 and *CYP2C18* had trends with
330 decreased editing, suggesting that these sites may be overall less effective at the on-target, potentially due
331 to competing off-targets (Figure 6). We conclude from this that on-target editing was successful in all
332 conditions except prime editing, with highly variable frequencies as may be expected without substantial
333 optimization.

334 **Comparative analysis of DSB editors in HEK293-Cas9 and HSPCs (off-target)**

335 A range of nominated off-targets for the six gRNAs were selected from two orthogonal methods for
336 downstream confirmation: UNCOVERseq nominations and *in silico* nominations. A range of 26 to 201
337 putative editing sites were interrogated per multiplexed amplicon rhAmpSeq panel with an UNCOVERseq:*in*
338 *silico* nomination origin split ranging from 53.8% to 100% for the interrogated target lists (Figure 6E). Panels
339 were sequenced with a goal of at least reaching 1,000x coverage per off-target to ensure adequate
340 sensitivity for calling significantly edited off-targets. Sequencing the six panels demonstrated we were able
341 to achieve a median read coverage ranging between 34,000x to 76,000x, with consistency in coverage
342 between edited and corresponding control samples (Supplementary Figure 7A). The number of off-targets
343 reaching sufficient coverage (>1,000x) ranged from 92% to 100% per panel, with a range of 0 to 15 targets
344 not being at sufficient coverage per panel (Supplementary Figure 7B).

345 To determine the frequency of UNCOVERseq HEK293-Cas9 nominations that convert to
346 empirically edited sites in variable DSB editing contexts, we compared this frequency for *S.p.* Cas9 both in
347 HEK293-Cas9 and HSPCs (HiFi Cas9). For HEK293-Cas9, a range of 54.5% of nominated off-targets all
348 the way to 100% of off-targets had confirmed editing ranging from to 0.02% to 95% indel editing,
349 demonstrating the true positive rate for UNCOVERseq-nominated sites remains high even with only a single

350 replicate in the appropriately paired confirmation context (Figure 6F; Supplementary Figure 8A-F). For
351 HSPCs, a range of 2.4% to 34.5% of nominated targets were successfully confirmed per gRNA, with
352 confirmed indel editing ranging from 0.06% to 88% (Figure 6F; Supplementary Figure 9A-F).
353 Nomination:confirmation frequencies trended to increase as gRNA specificity decreased, suggesting that
354 the method is still successfully nominating relevant off-targets, but that these sites likely no longer exceed
355 detectable frequencies or are no longer edited in the higher genome editing specificity context of HSPCs
356 delivered a HiFi Cas9 mRNA editor (Figure 6F). Furthermore, at higher gRNA specificities the only
357 nominated target being confirmed is the on-target site for HiFi Cas9 in HSPCs (Supplementary Figure 9A-
358 F).

359 Off-targets that were confirmed were compared to the list of those that would have been dropped
360 given a different previously evaluated alignment method (Regex method; Figure 1). A range of 3 to 23 bona
361 fide off-targets per gRNA in HEK293-Cas9 were successfully nominated using our alignment method that
362 were missed using GUIDE-seq analysis Regex method, with a range of observed indel editing from 0.02%
363 to 68% (Supplementary Figure 10A). In HSPCs, 1 bona fide HiFi Cas9 off-target was identified with a
364 frequency of 0.01% with our alignment method that was missed using the Regex alignment method
365 (Supplementary Figure 10B). This demonstrates that DSB off-target sites that were nominated due to
366 differences in alignment criteria can result in bona fide off-target indel editing in both HEK293-Cas9 and
367 HSPCs.

368 **Comparative analysis of non-DSB editors in HSPCs (off-target)**

369 Off-target were simultaneously confirmed for both indel and base editing in the non-DSB treatments
370 for HSPCs (ABE and CBE). Similarly, we interrogated the frequency that UNCOVERseq HEK293-Cas9
371 nominations convert to empirically edited sites in HSPCs being delivered a base editor. For ABE treatments,
372 a range of 2.4% to 29% of nominated targets had confirmed editing ranging from 0.53% to 75.9% cumulative
373 ABE editing (Figure 6G-H; Supplementary Figure 11A-F). For CBE treatments, a range of 2.4% of
374 nominated targets to 14.5% of targets had confirmed editing ranging from 0.51% to 32.9% CBE editing
375 (Figure 6G; Figure 6I; Supplementary Figure 12A-F). Significant indel editing was observed for all ABE and
376 CBE editing treatments, with largely only the on-target gRNA containing indels at higher specificity gRNAs

377 (Figure 6C; Supplementary Figure 13A-F; Supplementary Figure 14A-F). Off-target indel frequencies for
378 ABE treatments ranged from 0.02% to 0.88% indels across different gRNAs (Supplementary Figure 13A-
379 F). Interestingly, three off-target sites were found to generate indel events at the higher specificity *TRAC7*
380 gRNA under ABE treatment conditions, which lacked any significant off-targets in paired DSB Cas9
381 treatment (Supplementary Figure 13D). Off-target indel frequencies for CBE treatments ranged from 0.08%
382 to 0.66% indels across different gRNAs (Supplementary Figure 14A-F). Generally, it was observed that
383 indel and base editing frequencies were lower in CBE-treated samples in comparison to ABE-treated
384 samples (Figure 6I-J; Supplementary Figure 11A-F; Supplementary Figure 12A-F), although this could be
385 a result of lower overall activity of the base editor instead of off-target propensity.

386 When comparing the list of confirmed ABE/CBE off-targets to those that would have been excluded
387 given a different alignment method during nomination we found 1 bona fide off-target of the *PDCD1* gRNA
388 that was identified for both ABE and CBE treatments with a frequency range of 0.5% to 3.1% base editing
389 that was missed using the Regex alignment method (Supplementary Figure 10B). This demonstrates that
390 off-target sites that were nominated due to differences in alignment criteria can also result in bona fide off-
391 target base editing activity for both ABE and CBE editors in HSPCs.

392 To investigate relationships between DSB indels, SSB indels, and base editing, we binned
393 confirmed base editing off-targets based on their presence of indels in either DSB or SSB systems. Base
394 editing with the highest frequencies (median 20.6% and 2.3% for ABE and CBE, respectively), were found
395 to coincide with indel editing for both DSB and SSB systems (Figure 6H). Interestingly, only ABE treatments
396 were found to have an increased frequency of base editing at SSB only sites, with eight detected SSB-only
397 off-targets with a median 13.1% cumulative base editing compared to zero sites for CBE (Figure 6). This
398 may coincide to activity differences, as both ABE editing/indel activity was generally higher than CBE
399 editing/indel activity across the different sites (Supplementary Figure 11-14). DSB-only and sites with no
400 evidence of significant indel editing were present in confirmed sites for both ABE and CBE treatments, albeit
401 with lower median cumulative base editing frequencies (Figure 6). The on-target indel and base editing
402 activity of the different gRNAs were rank-order correlated (r=0.66 - 0.89), suggesting that indel editing
403 frequencies may be predictive of base editing frequencies (Supplementary Figure 15). Similarly, off-target

404 DSB indel editing frequencies from HiFi Cas9 demonstrated rank-order correlation with off-target base
405 editing frequencies (r = 0.77 – 0.78) at sites that had significant DSB indel editing frequencies in HSPCs
406 (Figure 6J). This provides evidence that DSB editing may be indicative of base editing activity, meaning
407 that DSB-nominated sites are meaningful for interrogation in the context of both indel and base editing off-
408 target assessment for both ABE and CBE modalities.

409 **Comparative translocation analysis and overall editing burden across editing modalities**

410 To investigate differential frequencies of editor modalities to generate large structural variants
411 (>0.1% frequencies) in HSPCs, we investigated the previously described six sites for on-target:off-target
412 and off-target:off-target translocations using amplicon sequencing. Only the *PDCD1* gRNA had detectable
413 translocations, with two out of three of the translocations being shared between the *S.p.* Cas9 and ABE
414 conditions (Figure 7A). Shared translocations included a fusion of OTE132 to OTE94 and OTE160 to
415 OTE158, with comparable average frequencies ranging between 1.0% - 1.7% and 0.3% - 0.5%,
416 respectively (Figure 7A). The overall estimated translocation burden for this gRNA was estimated to be an
417 average of 1.4% translocations for *S.p.* Cas9 and an average of 2.2% translocations for ABE conditions
418 (Figure 7A). This suggests that translocations are either below 0.1% or not occurring in healthy HSPC
419 donors across higher gRNA specificities. However, it is noteworthy that they are still occurring for both SSB
420 and DSB modalities, as has been previously observed[39].

421 When calculating the normalized risk of cumulative off-target frequencies (indels, base edits, and
422 translocations) across editor modalities throughout our spectrum of gRNA specificities, off-target ratios were
423 observed for the *PDCD1* gRNA over a range 9.4 – 89.0 off-target events per 1 on-target event (Figure 7B).
424 Off-target ratios for the *CYP2C18* gRNA ranged from 0.07 – 0.76 off-target events per 1 on-target event
425 (Figure 7B). Trends consistently showed that overall off-target burden of DSB editors was actually
426 decreased in comparison to SSB base editors for the cumulative frequency of event types monitored using
427 this strategy (Figure 7B). Even though the *B2M* gRNA was considered higher-specificity, a single significant
428 ABE off-target was observed for this treatment contributing to a higher ratio (Figure 7B). This highlights that
429 even higher-specificity gRNAs may generate observable off-targets in clinically relevant cell types.

430

431 **Discussion**

432 Our study presents an improved, end-to-end characterized *in cellulo* method for the nomination of
433 off-target sites in CRISPR experiments that we collectively refer to as UNCOVERseq (v1.0). This method
434 leverages several technological improvements to collectively streamline the *in cellulo* nomination process,
435 improve NGS data quality, and increase the number of high-confidence nominated sites through
436 computational analysis improvements compared to other previously published methods. By demonstrating
437 recommended operational conditions that can allow the experiments to be performed independent of cell
438 context with controls grounded in empirical data, we provide a framework to ensure translation to different
439 treatment modalities with quantifiable levels of performance from experiment to experiment. Furthermore,
440 we demonstrate the workflow is capable of nominating relevant unique and shared off-targets for both DSB-
441 based and SSB-based CRISPR editing systems and demonstrate correlations between DSB formation and
442 the frequency of a site to be edited by ABE/CBE editors.

443 To ensure all relevant off-targets are assessed, high analytical sensitivity is a critical off-target
444 nomination metric. However, accurate calculations of false-negative rates from nomination methods have
445 been challenged by technical difficulties in obtaining an empirically defined gold-standard of all true-positive
446 off-targets. Previous work has led to a perception that *in vitro* biochemical methods are inherently more
447 sensitive than *in cellulo* methods as evidenced by: 1) true positive sites captured by *in vitro* methods like
448 CHANGE-seq that are missed with GUIDE-seq and 2) multiple accounts of *in cellulo* methods being largely
449 a subset of *in vitro* results[6,7]. To reduce risk of false negatives, we demonstrate a strategy for *in cellulo* off-
450 target nomination using UNCOVERseq where high gDNA input and promiscuous editing conditions are
451 used to greatly amplify nomination signal to reproducibly detect sub-0.05% editing events while still
452 retaining sites derived from higher fidelity modalities and primary cell lines. Using UNCOVERseq, we
453 demonstrate that previously published accounts of *in cellulo* methods were not as sensitive as
454 UNCOVERseq. However, it is not clear whether this is due to insufficient operational conditions (read depth,
455 library complexity, etc.) to maximize capabilities of many assays as opposed to the technical improvements
456 that confer enhanced nomination capabilities to UNCOVERseq. We also find that *in vitro* biochemical
457 assays do not sensitively cover the full range of putative true positive lists generated from highly reproduced

458 UNCOVERseq nomination. This provides evidence counter to claims that *in vitro* methods are inherently
459 more sensitive for off-target nomination. Future work should look to further expand gRNAs
460 nominated/confirmed and provide empirical knowledge on the optimal operating conditions for different
461 assays.

462 Precision is another important metric for off-target nomination methods to appropriately select sites
463 for downstream confirmation. Some methods for off-target nomination can lead to thousands of sites being
464 nominated with low precision which is cost-prohibitive for downstream interrogation given the high coverage
465 depth required for sensitive off-target confirmation. Using UNCOVERseq with sufficient replication ($\geq$3
466 replicates), we demonstrate that true positives can be obtained from nomination that may approach 100%
467 precision, enabling rapid identification of sites for benchmarking methods. We additionally demonstrate that
468 UNCOVERseq nomination frequencies strongly correlate to observed editing frequencies, and that
469 biochemical *in vitro* methods generally lack as strong of a correlation as compared to *in cellulo* and *in situ*
470 methods. This is an important feature enhancing method-specific site prioritization, as strong correlations
471 to observable frequencies enable better prioritization or filtering of large site lists. Future work should look
472 to better confirm this logic by performing targeted sequencing on more confirmable sites with different levels
473 of reproducibility.

474 Using a simple prioritization method based on frequency, replication, and high-level indicators of
475 risk (exonic regions vs. intergenic, etc.), we demonstrate UNCOVERseq nominations with recommended
476 experimental structures can result in manageable confirmation panel sizes for downstream confirmation
477 (e.g., <250 sites across a range of specificities). We demonstrate that replicates are important in the off-
478 target nomination process to ensure that sites meeting basic prioritization criteria are appropriately
479 identified, with >25% of putative targets being missed without use of biological replicates. However, to better
480 understand risk after off-target nomination and confirmation across methods, a more standardized scoring
481 system to prioritize off-targets is needed in the future. The fields of oncology and heritable diseases have
482 encountered similar issues and derived guidelines including tiered scoring systems from the American
483 College of Medical Genetics (ACMG) and Association of Molecular Pathology (AMP) and modifications
484 leveraging these criteria[21,40,41]. Gene editing may be able to leverage some of these learnings, but will face

485 unique challenges in categorization of off-target risk since even off-targets in intergenic space during the
486 nomination phase can be at risk for known structural variations derived from DSBs and SSBs. This includes
487 events such as translocations[42], loss of heterozygosity[43] (LoH), aneuploidy[44], and other large variants like
488 multi-kilobase deletions[45]. Given this, it seems likely that probability, frequency, and even proximity to other
489 coding regions will be important criteria for triaging off-targets for assessment. In agreement with previous
490 findings, we find that *in cellulo* methods provide a much stronger relationship between frequency of off-
491 targets nominated and observed compared to *in vitro* methods. This highlights that *in cellulo* methods like
492 UNCOVERseq may have additional utility in future risk scoring criteria given their ability to be predictive of
493 observable frequencies

494 Benchmarked nomination and confirmation methodologies are needed for both DSB and SSB-
495 based editing modalities. By selecting a variable range of gRNA specificities, we demonstrate that even in
496 popular *ex vivo* models like HSPCs with mRNA delivery, high specificity gRNAs are still sensitive to both
497 SSB indels and base editing off-target effects at frequencies >0.01% and 0.5%, respectively. Furthermore,
498 we demonstrate that indel editing and base editing are rank-order correlated across 34 base editing on/off-
499 targets, supporting the idea that DSB-based nomination methods are effective tools for nominating both
500 indel and base editing activity. Base editing-specific nomination methods, such as CHANGE-seq-BE, have
501 been developed to target base editing events, while demonstrating unique off-target confirmation findings[46].
502 It is our belief that orthogonal methods for nominating both base editing events and indel events are likely
503 needed for the foreseeable future, especially given some of our findings that some UNCOVERseq-
504 nominated sites generate confirmable indels only in conditions using the SSB base editing modalities in
505 translational cellular contexts.

506 We envision UNCOVERseq coupled with promiscuous conditions being a powerful tool to help
507 sensitively identify CRISPR-Cas off-targets for interrogation during pre-clinical development phases. By
508 enhancing the quality of off-target nomination and grounding NGS operational conditions in empirical data,
509 we believe that UNCOVERseq improves informed risk assessment of gene editing in translational systems.
510 Furthermore, by detailing inner-workings and described process controls for UNCOVERseq, we hope to

511 enable more flexibility and standardization for the necessary technologies required to operate off-target
512 safety assessment workflows in both research and commercial spaces.

513 **Methods**

514 **Human cell culture and transfection (K562 and HEK293-Cas9)**

515 K562 (ATCC) and HEK293-Cas9 (ATCC) cells were cultured in Iscove's Modified Dulbecco's
516 Medium (IMDM; ATCC) and Eagle's Minimum Essential Medium (EMEM; ATCC) supplemented with 10%
517 FBS at 37°C with 5% CO_2. Ribonucleoprotein (RNP) complexes were formed by mixing Alt-R™ *S.p.* Cas9
518 Nuclease V3 (IDT) or SpyFi™ Cas9 Nuclease (Aldevron) and Alt-R CRISPR-Cas9 sgRNA (gRNA, IDT),
519 and incubating for 20 minutes at room temperature (Molar Ratio: 1:1.2, Cas9:gRNA). For each transfection,
520 8.0 x 10^5 cells were washed with 1X phosphate-buffered saline, resuspended in 20 µL of solution SF
521 (Lonza). For K562 cells, RNP complexes at 4 µM were combined with 4 µM of the dsODN (Supplementary
522 Table 1) into the SF solution, while for the HEK293-Cas9 cells, 5 µM gRNA and 0.5 µM dsODN were added
523 to the SF solution. This mixture was transferred into 1 well of a 96-well Nucleocuvette plate (Lonza) and
524 electroporated using program FF-120 (K562) or DS-150 (HEK293-Cas9). Two nucleofections per replicate
525 were performed and each treatment done in triplicate. Following electroporation, cells were transferred to
526 a 6-well plate preheated with either IMDM or EMEM and were incubated at 37°C with 5% CO_2 for 72 hours.
527 After incubation, genomic DNA (gDNA) was extracted using either the Purelink™ Pro 96 Genomic DNA
528 Purification kit or the Monarch™ Spin gDNA Extraction Kit (New England Biolabs) according to the
529 manufacturer's instructions, eluted in low-EDTA TE buffer (IDT, 11-05-01-05), and quantified using a
530 NanoDrop 8000 UV-Vis Spectrophotometer (ND-8000-GL).

531 **Primary T-cell culture and transfection**

532 Frozen human primary pan-T cells (STEMCELL Technologies) from 2 unique human donors were
533 thawed in ImmunoCult-XF T Cell Expansion Medium including 300IU IL-2 (Cytiva) and activated with 10
534 µL/mL TransAct, human, T cell activator (Miltenyi Biotec) for 48 hours. To prepare for transfection using
535 Lonza 96-well plate 4-D Nucleofector system, cells were counted, pelleted using centrifugation (300 x g, 10
536 minutes at room temperature), and washed gently with 10 mL 1X phosphate-buffered saline. Cells were
537 again pelleted and resuspended in Lonza Nucleofection Solution P3 at 2.5 x 10^6 cells/mL. For each
538 electroporation, 5 µL of RNP complex and 3 µL dsODN was added to 20 µL of cells in P3 (5 x 10^5

539 cells/nucleofection) for a final concentration of 4 μM RNP (1:1.2 ratio of Cas9 to gRNA) and 1-4 μM dsODN.
540 Where tag was not included, 3 μL of IDT Alt-R Cas9 Electroporation Enhancer was added for 3 μM final
541 concentration to achieve a fixed final nucleofection reaction volume of 28 μL. Each reaction was mixed by
542 pipetting and 25 μL was transferred to an electroporation cuvette plate. The cells were electroporated
543 according to the manufacturer's protocol using the Amaxa 96-well Shuttle and nucleofection protocol 96-
544 EH-140. After electroporation, the cells were resuspended in 75 μL pre-warmed IL-2 culture media in the
545 electroporation cuvette. Triplicate aliquots of 25 μL of recovered cells were further cultured in 175 μL pre-
546 warmed IL-2 media with TransAct. Cells were incubated for 72 hours, after which gDNA was isolated and
547 quantified.

548 **iPSC culture and transfection**

549 iPSCs from fibroblasts (Coriell Institute, GM23338) were cultured in mTeSR™ Plus media (Stemcell
550 Technologies) at 37°C with 5% CO_2. RNPs were formed as described above. For transfection using Lonza
551 96-well plate 4-D Nucleofector system, cells were detached using ReLeSR™ (Stemcell Technologies) and
552 washed with 1X phosphate-buffered saline. Cells were resuspended in P3 buffer at 2 x 10^5
553 cells/nucleofection. CRISPR reagents at required final concentrations (4 μM RNP; 0.5 μM dsODN) were
554 added to the mix to make a final volume of 25 μL, and of which 20 μL was transferred to the nucleocuvette
555 for electroporation. The nucleovette plate was electroporated using code CA-137. After the nucleofection,
556 cells were recovered and plated in complete mTeSR Plus medium with 1X CloneR™ 2 supplement
557 (Stemcell Technologies). Recovery media was added to the electroporated cells to achieve a final volume
558 of 100 μL, and 25 μL of this was added to 175 μL media per replicate well for final plating in a vitronectin-
559 coated 96-well plate. During recovery and growth at 37°C with 5% CO_2 for up to 96 to 120 hours, media
560 changes were performed as desired and/or following manufacturer's protocols for media and CloneR 2
561 supplement. gDNA extraction and quantification was performed as described above.

562 **Off-target Nomination with UNCOVERseq**

563 500 ng of purified gDNA was enzymatically fragmented and adapter-ligated using the xGen™ DNA
564 Library Prep EZ UNI kit along with the xGen Deceleration Module (IDT, xGen DNA Library Prep EZ UNI 96
565 rxn, 10009822; xGen Deceleration Module 96 rxn, 10009823) according to the manufacturer's instructions
566 and cleaned with AMPure XP beads (Beckman). Following fragmentation and adapter ligation, rhPCR was

567 performed using rhAmpSeq™ Library Mix 1 (IDT) to amplify the DNA in a single tube using a forward primer
568 specific to the P5 adapter, a reverse primer specific for top and bottom strand of the integrated dsODN tag,
569 and an adapter-blocking oligo corresponding to each strand of the dsODN[31]. Following PCR, samples were
570 diluted 1:40 with nuclease-free water and used in a second PCR with rhAmpSeq™ Library Mix 2 (IDT) that
571 added a unique P7 adapter to each library. Libraries were then cleaned with AMPure XP beads and run on
572 an Agilent Fragment Analyzer for library quality assessment. All libraries were quantified with the Qubit 1X
573 dsDNA HS Assay kit (Invitrogen) and pooled in equimolar amounts. All libraries were sequenced using an
574 Illumina MiSeq or NextSeq2000 instrument with 150-bp paired-end reads. All oligonucleotides used in
575 preparation of UNCOVERseq libraries are listed in Supplementary Table 1.

576 **Vector Construct and *in vitro* transcription of modified mRNA**

577 Genes encoding HiFi Cas9[47], ABE8e[37], AncBE4max[36], and PE2[28] were each cloned into a plasmid
578 vector with a dT7 promotor followed by a 5'UTR, Kozak sequence, ORF, and 3'UTR for subsequent in vitro
579 transcription. Chemically modified Cas9, ABE8e, AncBE4max and PE2 mRNA was transcribed *in vitro* from
580 the PCR templates with full substitution of uridine by N^1-methylpseudouridine. Co-transcriptional capping
581 was achieved using CleanCap AG analog (TriLink), yielding a 5′ Cap 1 structure. Transcription reactions
582 were carried out with the HiScribe T7 High Yield RNA Synthesis Kit (New England Biolabs) in 0.5×
583 transcription buffer supplemented with 4 mM CleanCap AG. Following synthesis, mRNAs were purified
584 using the Monarch Spin RNA Cleanup Kit (New England Biolabs). PCR templates incorporated mammalian-
585 optimized UTRs (TriLink) and a 120-nucleotide poly(A) tail.

586 **HSPC culture and transfection**

587 $CD34^+$ HSPCs from a single human donor (Fred Hutch Cancer Center, RO04089) were cultured at
588 1×10^5 cells/mL in StemSpan SFEM II medium supplemented with 100 ng/mL SCF, 100 ng/mL TPO, 100
589 ng/mL FLT3L, 100 ng/mL IL-6, 20 µg/mL streptomycin, and 20 U/mL penicillin. Cultures were maintained at
590 37 °C in a humidified incubator with 5% CO_2. For electroporation, Cas9 mRNA and gRNA were mixed at a
591 1:1 weight ratio (3 µg each per reaction). ABE, CBE, and PE2 mRNAs were used at equimolar amounts to
592 Cas9 (3.4 µg ABE, 4 µg CBE, and 6 µg PE2), and pegRNA was added at the same molar amount as gRNA
593 (4.2 µg). HSPCs were resuspended in 20 µL Lonza P3 buffer and electroporated using a Lonza 4D-

594 Nucleofector (program DZ-100). After electroporation, cells were plated at 1 × 10^5 cells/mL in HSPC
595 medium.

596 **Computational Analysis – Nomination**

597 Following NGS, Illumina adapters and UMIs were identified and annotated using Picard
598 MarkIlluminaAdapters. Tag sequences were identified and trimmed using Cutadapt v4.2[48]. Sequencing
599 reads were aligned to hg38 (GRCh38.p12) reference genome using BWA mem[49] v0.7.15 and UMI
600 consensus reads were generated based on consensus from a single-strand (minimum UMI consensus size
601 = 1) using fgbio v0.7.0 (https://github.com/fulcrumgenomics/fgbio). Nomination of candidate off-target sites
602 began by using mapped UMI consensus reads to create a flanked search space (+/- 40 bp) to perform
603 alignment between the guide and empirical target region using a glocal implementation of the Needleman-
604 Wunsch alignment[50,51]. After a candidate match to the gRNA spacer region was identified in the sequencing
605 data, nominated off-target sites were identified using a hypergeometric test with multiple testing correction
606 (Benjamini & Hochberg; FDR<0.05) by comparing individual treatment samples and pooled control samples
607 for significant differences in representation between the two. We used the following criteria to nominate off-
608 target sites from this analysis for verification: 1) at least one sample nominated a given site with NGS
609 evidence on both sides of the cut site, 2) Levenshtein distance < 7 as determined post-alignment, and 3)
610 significant adjusted p-value when comparing the frequency of the event to the pooled control(s). Nominated
611 on/off-target sites had additional meta-data added based on alignment/genomic context and were placed
612 into described Tiers based on this meta-data (Supplementary Table 2).

613 **Library Preparation – Confirmation**

614 Genomic DNA was extracted from control and genome-edited cells as described above. Libraries
615 for amplicon NGS were prepared using a previously described rhAmpSeq amplification-based method (IDT)
616 using 100 ng of gDNA input[52]. Briefly, the first round of PCR was performed using target-specific primers.
617 A second round of PCR was used to incorporate P5 and P7 Illumina adapters to the ends of the amplicons
618 for universal amplification. Libraries were purified using Agencourt AMPure XP system (Beckman Coulter,
619 Brea, CA, USA) and quantified by quantitative PCR (qPCR) before sequencing on the Illumina MiSeq
620 platform (v.2 chemistry, 150-bp paired end reads; Illumina). Read demultiplexing was performed on the

621 resulting BCL files using Picard v2.18.9 (https://github.com/broadinstitute/picard)
622 IlluminaBasecallsToFastq.

623 **Computational Analysis – Confirmation**

624 Analysis of the sequencing data to identify confirmed off-target editing at the nominated sites was
625 performed using CRISPAltRations v1.2.1[53]. This analysis comprised two parallel workflows: identification
626 of indels at the position of the DSB/SSB, and identification of base editor-induced A->G (ABE) or C->T
627 (CBE) transversions in the relevant base-editing window.

628 For identifying indels, the window for event quantification was centered on the canonical cut site
629 and events quantified utilizing the default window size for Cas9 (8 bp). To determine whether indels found
630 in the sequencing data could result from bona fide off-target cleavage, indels were grouped by location
631 relative to the cut site (prioritizing minimum distance to cut site) followed by fitting counts of events to a
632 negative binominal model with a Wald test for significance in each location bin per off-target using the
633 DESeq2 package[35] within IDT's OTEasy tool (Schmaljohn et al., Manuscript in Preparation). For
634 classification of indel off-target editing, the tool requires: 1) sufficient read coverage for the site (>1,000x)
635 in all replicates, 2) significant edits to occur at or adjacent to the cut site after optimal alignment, 3) the
636 classified cumulative significant edits to exceed 0.01%, 4) the comparison of treatment/control samples at
637 the site to have a significant adjusted p-value ($p < 0.05$), and 5) an average coverage frequency of at least
638 5x the ascribed cumulative frequency observed (e.g., for 0.1% editing, at least 5,000x coverage). Blunt
639 dsDNA tag integration quantification for quality control analysis were classified by aligning quantified
640 insertions >10 bp in size from the CRISPAltRations output to the expected dsDNA tag using the biopython
641 implementation of the Needleman-Wunsch aligner[50]. Alignments with an alignment score greater than 50
642 were quantified as a tag integration event, and events were considered imperfect if any base was mutated
643 or missing from the expected dsDNA sequence alignment.

644 For identifying base editing-generated off-target effects, the window for event quantification was
645 centered in the middle of canonical base-editing window between position +5/+6 of the spacer (5' to 3') with
646 a 5 bp window for quantification. To determine significant base-editing transitions resulting in off-target
647 editing, all individual events that contained an ABE (A>G or T>C) or CBE (C>T or G>A) transition were

648 grouped according to unique base editing events in the window and fitting counts of events to a negative
649 binominal model with a Wald test for significance in each location bin per off-target using the DESeq2
650 package[54] within IDT's OTEasy tool (Schmaljohn et al., Manuscript in Preparation). For classification of
651 adenine base editing at off-targets, the tool requires: 1) sufficient read coverage for the site (>1,000x) in all
652 replicates, 2) the classified cumulative significant edits to exceed 0.5%, 3) the comparison of
653 treatment/control samples at the site to have a significant adjusted p-value ($p < 0.05$), and 4) an average
654 coverage frequency of at least 5x the ascribed cumulative frequency observed.

655 **Computational Analysis – Translocations**

656 To quantify translocations from editing, Primer Anchored Statistical Translocation Analysis (PASTA)
657 was used (Kurgan et al., Manuscript in Preparation). This analysis is only performed on the amplicon
658 sequencing pools containing the on-target edit (because multiplexed amplification is a requirement for event
659 detection using the method), and reactions not containing the on-target edit are unlikely to have any
660 significant translocation events. To quantify translocations, expected primers were identified in reads using
661 fg-idprimer (https://github.com/fulcrumgenomics/fg-idprimer; -k=6, -K=8, -S=5, --max-mismatch-rate=0.07).
662 Following this, treatment/control pairs had their counts paired and primer count frequencies subjected to a
663 one-tailed hypergeometric test with Benjamini-Hochberg correction (statsmodel v0.15.0; default settings)
664 to calculate an adjusted p-value (p-adj). Unexpected primer pairs with padj < 0.01 with no flags were
665 classified as a translocation and had the translocation frequency (P) calculated using the following equation:

666 $$P_t = \frac{n_t}{f_{total}} + \frac{n_t}{r_{total}}$$

667 Where 'n' is equal to the count of the unexpected primer pair of interest, 't' is the significant
668 translocation being interpreted, 'f' is the total count of the shared forward primer events excluding the count
669 participating in the 'n' translocation event, and 'r' is the total count of shared reverse primer events excluding
670 the count participating in the 'n' translocation event. The translocation frequency is then adjusted by the
671 background level frequency in the control by subtracting any translocation frequency observed in the control
672 sample from the treatment frequency. Total translocation burden (B) was calculated using the following
673 equation:

674 $$B = 1 - \prod_{t}^{t_n}(1 - P_t)$$

675 Where ‘t’ is equal to a significant translocation, and ‘tn’ is equal to the last significant translocation
676 of all translocations. All translocations for the purposes of this equation are assumed to be occurring
677 independently. Using the method, translocations are quantified if: 1) the estimated frequency exceeds 0.1%
678 of editing, 2) the translocation has a significant p-value ($p < 0.01$), and 3) the translocation is found to meet
679 these criteria in all replicates.

680 **Data Availability Statement**

681 Data generated and analyzed during this study using the UNCOVERseq method are available for download.
682 These datasets are provided exclusively for **non-commercial research purposes**. Use of the data for any
683 commercial applications—including but not limited to training or developing predictive models, designing
684 tools for gene editing applications, or integrating into commercial software or services—is strictly prohibited
685 without prior written permission from the authors. This restriction applies retroactively to all versions of the
686 datasets provided in this work, including those downloaded prior to the publication of this statement. Users
687 who have previously accessed the data are requested to comply with these updated terms and refrain from
688 any commercial use, without prior written permission.

689 **Disclaimers and Conflicts of Interest**

690 Products and tools supplied in this manuscript by IDT are for research use only and not intended for
691 diagnostic or therapeutic purposes. Purchaser and/or user are solely responsible for all decisions regarding
692 the use of these products and any associated regulatory or legal obligations. For informational use only.
693 The data provided are for informational use only and should not be used as the sole basis for any critical
694 decision making. The data generated are based on assay procedures that have not undergone full
695 validation: formal design and development activities are on-going. K.J.K., B.T., M.L.S., G.L.K., S.C., R.C.,
696 E.S., T.O., K.M., A.S.P., H.Z., M.B., M.M., S.W., R.T., G.R., and A.M.J. are employees of IDT, which offers
697 reagents and services for sale similar to some described in the manuscript. M.K.C. has equity in Kamau
698 Therapeutics.

699 **References**

700 1. Jinek, M. *et al.* A Programmable Dual-RNA–Guided DNA Endonuclease in Adaptive Bacterial
701 Immunity. *Science* **337**, 816–821 (2012).

702 2. Wang, J. Y. & Doudna, J. A. CRISPR technology: A decade of genome editing is only the
703 beginning. *Science* **379**, eadd8643 (2023).

704 3. Hsu, P. D. *et al.* DNA targeting specificity of RNA-guided Cas9 nucleases. *Nat Biotechnol* **31**,
705 827–832 (2013).

706 4. Fu, Y. *et al.* High-frequency off-target mutagenesis induced by CRISPR-Cas nucleases in human
707 cells. *Nat Biotechnol* **31**, 822–826 (2013).

708 5. Tsai, S. Q. *et al.* GUIDE-Seq enables genome-wide profiling of off-target cleavage by CRISPR-
709 Cas nucleases. *Nat Biotechnol* **33**, 187–197 (2015).

710 6. Tsai, S. Q. *et al.* CIRCLE-seq: a highly sensitive in vitro screen for genome-wide CRISPR–Cas9
711 nuclease off-targets. *Nat Methods* **14**, 607–614 (2017).

712 7. Lazzarotto, C. R. *et al.* CHANGE-seq reveals genetic and epigenetic effects on CRISPR–Cas9
713 genome-wide activity. *Nat Biotechnol* **38**, 1317–1327 (2020).

714 8. Cameron, P. *et al.* Mapping the genomic landscape of CRISPR–Cas9 cleavage. *Nat Methods* **14**,
715 600–606 (2017).

716 9. Kim, D. *et al.* Digenome-seq: genome-wide profiling of CRISPR-Cas9 off-target effects in human
717 cells. *Nat Methods* **12**, 237–243, 1 p following 243 (2015).

718 10. Dobbs, F. M. *et al.* Precision digital mapping of endogenous and induced genomic DNA breaks by
719 INDUCE-seq. *Nat Commun* **13**, 3989 (2022).

720 11. Cradick, T. J., Qiu, P., Lee, C. M., Fine, E. J. & Bao, G. COSMID: A Web-based Tool for
721 Identifying and Validating CRISPR/Cas Off-target Sites. *Molecular Therapy - Nucleic Acids* **3**, e214
722 (2014).

723 12. Bae, S., Park, J. & Kim, J.-S. Cas-OFFinder: a fast and versatile algorithm that searches for
724 potential off-target sites of Cas9 RNA-guided endonucleases. *Bioinformatics* **30**, 1473–1475 (2014).

725 13. Chaudhari, H. G. *et al.* Evaluation of Homology-Independent CRISPR-Cas9 Off-Target
726 Assessment Methods. *CRISPR J* **3**, 440–453 (2020).

727 14. Cromer, M. K. *et al.* Comparative analysis of CRISPR off-target discovery tools following ex vivo
728 editing of CD34+ hematopoietic stem and progenitor cells. *Mol Ther* **31**, 1074–1087 (2023).

729 15. Horlbeck, M. A. *et al.* Nucleosomes impede Cas9 access to DNA in vivo and in vitro. *Elife* **5**,
730 e12677 (2016).

731 16. Cancellieri, S. *et al.* Human genetic diversity alters off-target outcomes of therapeutic gene
732 editing. *Nat Genet* **55**, 34–43 (2023).

733 17. Jennings, L. J. *et al.* Guidelines for Validation of Next-Generation Sequencing–Based Oncology
734 Panels. *J Mol Diagn* **19**, 341–365 (2017).

735 18. Yang, Z.-X. *et al.* OliTag-seq enhances in cellulo detection of CRISPR-Cas9 off-targets. *Commun*
736 *Biol* **7**, 1–15 (2024).

737 19. Nobles, C. L. *et al.* iGUIDE: an improved pipeline for analyzing CRISPR cleavage specificity.
738 *Genome Biology* **20**, 14 (2019).

739 20. Shapiro, J. *et al.* Increasing CRISPR Efficiency and Measuring Its Specificity in HSPCs Using a
740 Clinically Relevant System. *Molecular Therapy - Methods & Clinical Development* **17**, 1097–1107 (2020).

741 21. Li, M. M. *et al.* Standards and Guidelines for the Interpretation and Reporting of Sequence
742 Variants in Cancer. *J Mol Diagn* **19**, 4–23 (2017).

743 22. Human Gene Therapy Products Incorporating Human Genome Editing; Guidance for Industry.

744 23. Zhang, L. *et al.* AsCas12a ultra nuclease facilitates the rapid generation of therapeutic cell
745 medicines. *Nat Commun* **12**, 3908 (2021).

746 24. Liu, G., Lin, Q., Jin, S. & Gao, C. The CRISPR-Cas toolbox and gene editing technologies.
747 *Molecular Cell* **82**, 333–347 (2022).

748 25. Zetsche, B. *et al.* Cpf1 is a single RNA-guided endonuclease of a class 2 CRISPR-Cas system.
749 *Cell* **163**, 759–771 (2015).

750 26. Gaudelli, N. M. *et al.* Programmable base editing of A•T to G•C in genomic DNA without DNA
751 cleavage. *Nature* **551**, 464–471 (2017).

752 27. Komor, A. C., Kim, Y. B., Packer, M. S., Zuris, J. A. & Liu, D. R. Programmable editing of a target
753 base in genomic DNA without double-stranded DNA cleavage. *Nature* **533**, 420–424 (2016).

754 28. Anzalone, A. V. *et al.* Search-and-replace genome editing without double-strand breaks or donor
755 DNA. *Nature* **576**, 149–157 (2019).

756 29. Newby, G. A. *et al.* Base editing of haematopoietic stem cells rescues sickle cell disease in mice.
757 *Nature* **595**, 295–302 (2021).

758 30. Arbab, M. *et al.* Base editing rescue of spinal muscular atrophy in cells and in mice. *Science* **380**,
759 eadg6518 (2023).

760 31. Dobosy, J. R. *et al.* RNase H-dependent PCR (rhPCR): improved specificity and single nucleotide
761 polymorphism detection using blocked cleavable primers. *BMC Biotechnol* **11**, 80 (2011).

762 32. Tian, R. *et al.* Massively parallel CRISPR off-target detection enables rapid off-target prediction
763 model building. *Med* **4**, 478-492.e6 (2023).

764 33. Yan, W. X. *et al.* BLISS is a versatile and quantitative method for genome-wide profiling of DNA
765 double-strand breaks. *Nat Commun* **8**, 15058 (2017).

766 34. Musunuru, K. *et al.* In vivo CRISPR base editing of PCSK9 durably lowers cholesterol in
767 primates. *Nature* **593**, 429–434 (2021).

768 35. Kim, D. & Kim, J.-S. DIG-seq: a genome-wide CRISPR off-target profiling method using
769 chromatin DNA. *Genome Res* **28**, 1894–1900 (2018).

770 36. Koblan, L. W. *et al.* Improving cytidine and adenine base editors by expression optimization and
771 ancestral reconstruction. *Nat Biotechnol* **36**, 843–846 (2018).

772 37. Richter, M. F. *et al.* Phage-assisted evolution of an adenine base editor with improved Cas
773 domain compatibility and activity. *Nat Biotechnol* **38**, 883–891 (2020).

774 38. Mathis, N. *et al.* Predicting prime editing efficiency and product purity by deep learning. *Nat*
775 *Biotechnol* 10.1038/s41587-022-01613–7 (2023) doi:10.1038/s41587-022-01613-7.

776 39. Fiumara, M. *et al.* Genotoxic effects of base and prime editing in human hematopoietic stem cells.
777 *Nat Biotechnol* **42**, 877–891 (2024).

778 40. Richards, S. *et al.* Standards and Guidelines for the Interpretation of Sequence Variants: A Joint
779 Consensus Recommendation of the American College of Medical Genetics and Genomics and the
780 Association for Molecular Pathology. *Genet Med* **17**, 405–424 (2015).

781 41. Tavtigian, S. V. *et al.* Modeling the ACMG/AMP Variant Classification Guidelines as a Bayesian
782 Classification Framework. *Genet Med* **20**, 1054–1060 (2018).

783 42. Ghezraoui, H. *et al.* Chromosomal translocations in human cells are generated by canonical
784 nonhomologous end-joining. *Mol Cell* **55**, 829–842 (2014).

785 43. Alanis-Lobato, G. *et al.* Frequent loss of heterozygosity in CRISPR-Cas9–edited early human
786 embryos. *Proceedings of the National Academy of Sciences* **118**, e2004832117 (2021).

787 44. Cullot, G. *et al.* CRISPR-Cas9 genome editing induces megabase-scale chromosomal
788 truncations. *Nat Commun* **10**, 1136 (2019).

789 45. Kosicki, M., Tomberg, K. & Bradley, A. Repair of double-strand breaks induced by CRISPR-Cas9
790 leads to large deletions and complex rearrangements. *Nat Biotechnol* **36**, 765–771 (2018).

791 46. Lazzarotto, C. R. *et al.* CHANGE-seq-BE enables simultaneously sensitive and unbiased in vitro
792 profiling of base editor genome-wide activity. 2024.03.28.586621 Preprint at
793 https://doi.org/10.1101/2024.03.28.586621 (2024).

794 47. Vakulskas, C. A. *et al.* A high-fidelity Cas9 mutant delivered as a ribonucleoprotein complex
795 enables efficient gene editing in human hematopoietic stem and progenitor cells. *Nat Med* **24**, 1216–1224
796 (2018).

797 48. Martin, M. Cutadapt removes adapter sequences from high-throughput sequencing reads.
798 *EMBnet.journal* **17**, 10–12 (2011).

799 49. Li, H. & Durbin, R. Fast and accurate short read alignment with Burrows-Wheeler transform.
800 *Bioinformatics* **25**, 1754–1760 (2009).

801 50. Pj, C. *et al.* Biopython: freely available Python tools for computational molecular biology and
802 bioinformatics. *Bioinformatics (Oxford, England)* **25**, (2009).

803 51. Needleman, S. B. & Wunsch, C. D. A general method applicable to the search for similarities in
804 the amino acid sequence of two proteins. *J Mol Biol* **48**, 443–453 (1970).

805 52. Jacobi, A. M. *et al.* Simplified CRISPR tools for efficient genome editing and streamlined
806 protocols for their delivery into mammalian cells and mouse zygotes. *Methods* **121–122**, 16–28 (2017).

807 53. Kurgan, G. *et al.* CRISPAltRations: a validated cloud-based approach for interrogation of double-
808 strand break repair mediated by CRISPR genome editing. *Mol Ther Methods Clin Dev* **21**, 478–491
809 (2021).

810 54. Love, M. I., Huber, W. & Anders, S. Moderated estimation of fold change and dispersion for RNA-
811 seq data with DESeq2. *Genome Biol* **15**, 550 (2014).

812

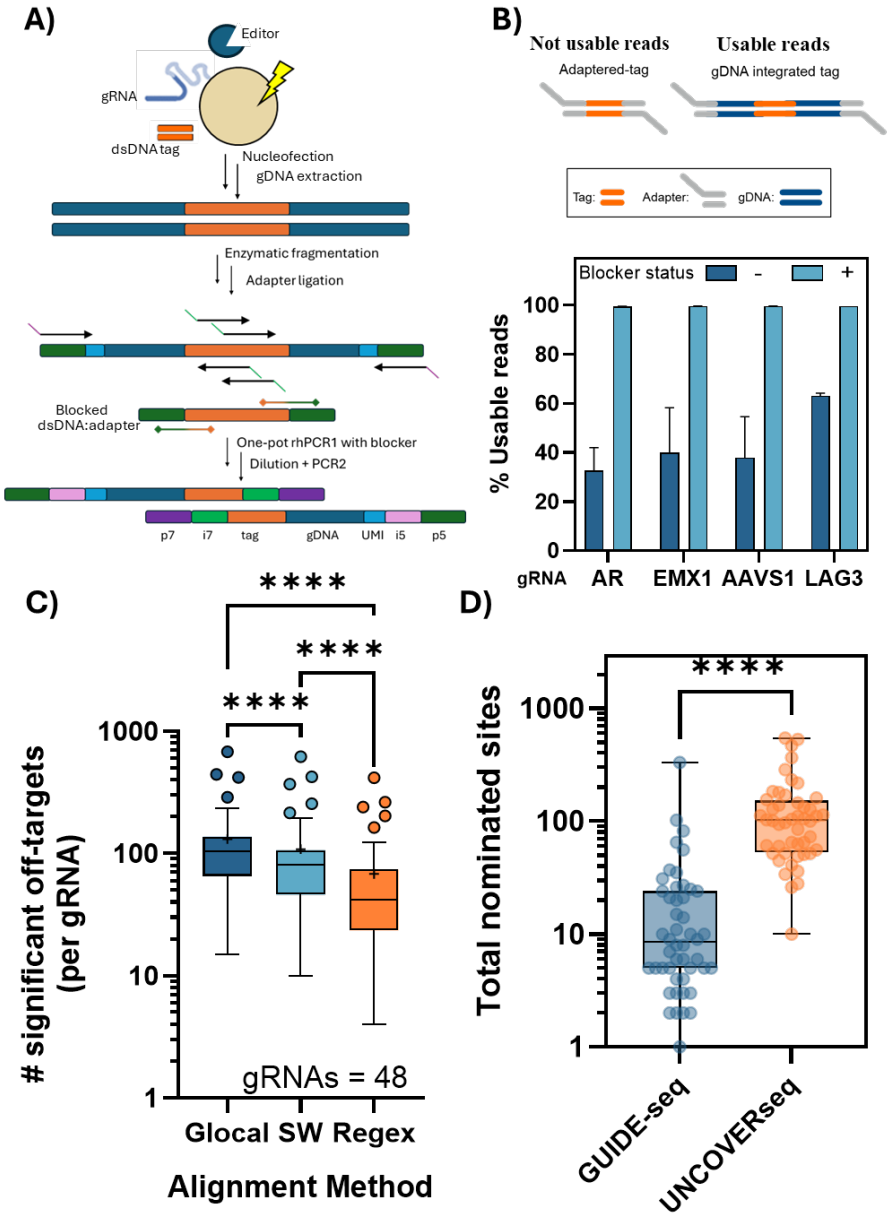

Figure 1. **Comparison of UNCOVERseq and the GUIDE-seq off-target nomination workflows. A)** An overview of the UNCOVERseq workflow demonstrates that cells with a genomically integrated dsDNA tag have gDNA extracted and amplified with rhPCR in a single reaction, with dsDNA tag:adapter byproducts being blocked by a targeted oligo before being sequenced and analyzed using our described workflow. **B)** A depiction is shown regarding what kind of events are targeted by the blocking oligo, with the usable reads (non-dsDNA:adapter reads) measured across nominated off-targets for 4 gRNAs in K562 (n = 3 per gRNA) with (light blue) or without (dark blue) the blocking oligo. **C)** Comparison of different alignment methods used in publicly available nomination packages was performed to determine differences in Levenshtein distance < 7 sites from a glocal Needleman-Wunsch alignment (Glocal; +2/-1/-10/-1 match/mismatch/gap open/gap extension), Smith-Waterman (SW; original GUIDE-seq pipeline; +2/-1/-100/-100 match/mismatch/gap open/gap extension) or string-match method (Regex; current GUIDE-seq pipeline). **D)** Tukey box plots show the end-to-end differences in total nominated off-target sites for the current GUIDE-seq method (wet lab protocol and Regex alignment) compared with UNCOVERseq. Data is representative of 48 gRNAs (Targets: *PDCD1, LAG3, CTLA4, NRP1, IL2RA*, and *TIGIT*; 8 gRNAs per target). Statistical significance was determined for pairwise comparisons using Wilcoxon matched-pairs signed rank test and for multiple comparisons using a Friedman test with a post-hoc Dunn's test with Bonferroni correction. ****$p < 0.0001$.

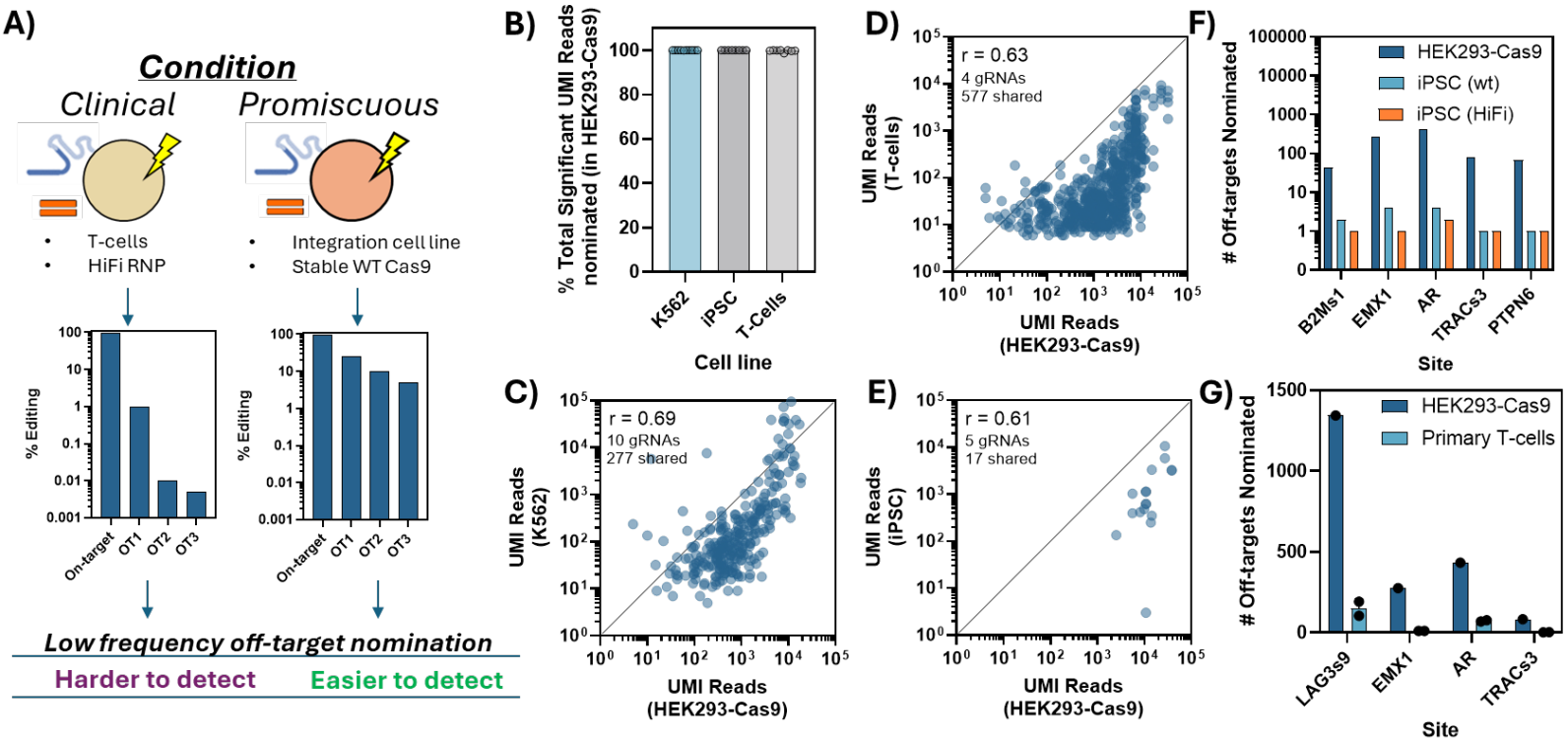

Figure 2. Analysis of performance of a promiscuous cell system and the ability to translate to other cellular systems. A) Example diagram demonstrating promiscuous nomination systems can help sensitively represent off-target lists by increasing the frequency that off-targets are detected. **B)** Comparison of total frequencies (represented as the cumulative % significant UMI reads) of nominated sites captured in a single replicate of HEK293-Cas9 vs. wildtype Cas9 RNP transfection using three different cell types: K562 (10 gRNAs; biological duplicates per gRNA), iPSCs (5 gRNAs; one biological replicate per gRNA; wildtype and HiFi Cas9), and primary T-cells (4 gRNAs; 2 biological replicates per gRNA as two different donors). Total UMI-corrected reads, total number of nominated sites, and Spearman correlation are shown for shared nominated sites between HEK293-Cas9 and, **C)** K562, **D)** T-cells, and **E)** iPSCs. Total number of nominated sites between **F)** iPSCs and **G)** primary T-cells are displayed in comparison to HEK293-Cas9.

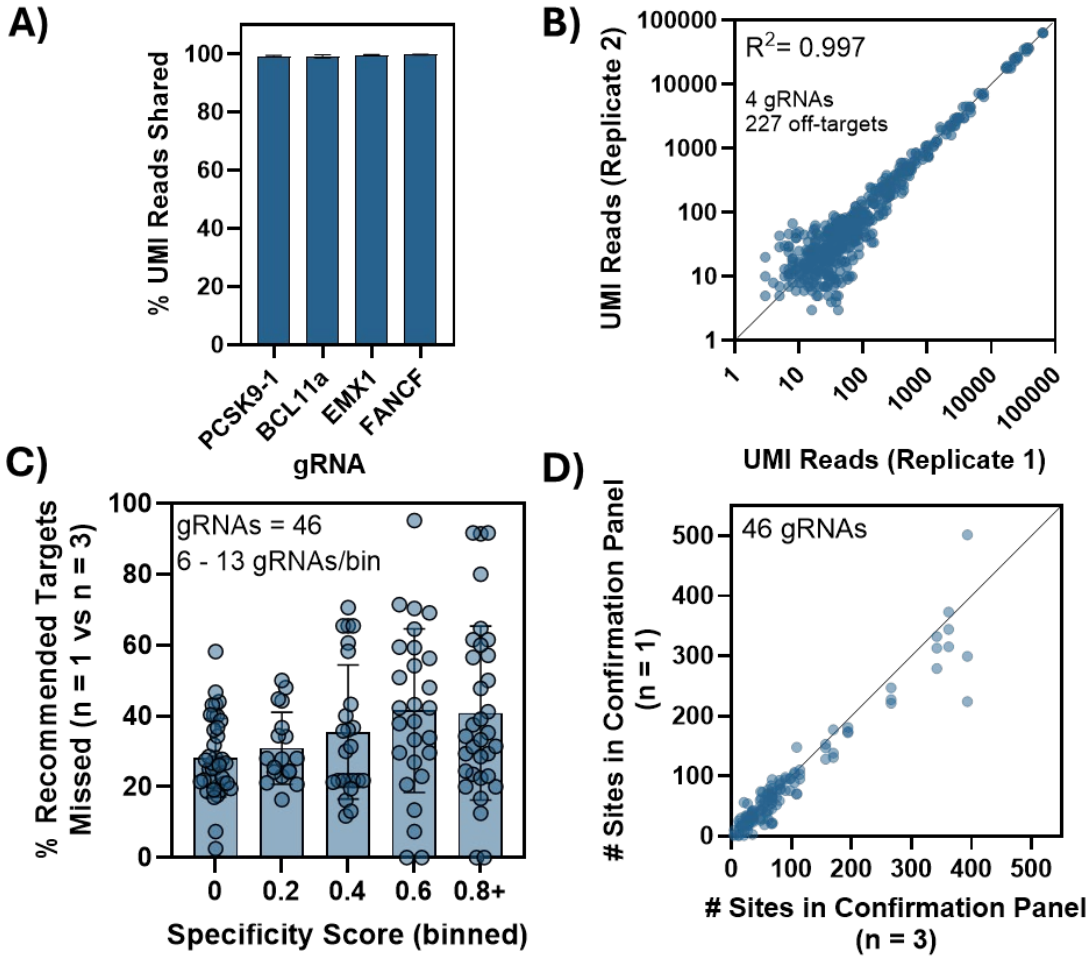

Figure 3. UNCOVERseq nomination reproducibility for high frequency and high priority off-targets. To measure the ability to reproducibly nominate off-targets at consistent frequencies, **A)** a combinatorial comparison of replicates was performed of targets nominated (by frequency, measured as cumulative UMI reads on overlapping targets / UMI reads on all nominated targets) using UNCOVERseq across 4 gRNAs in HEK293-Cas9 (n = 3 biological replicates per gRNA) and **B)** compared the target nomination frequency between replicates. To determine the reproducibility to capture high priority off-targets (defined as Tier 1 to Tier 3 in Supplementary Table 2) 46 gRNAs across a broad specificity score spectrum were nominated in triplicate in HEK293-Cas9 and **C)** the high priority panel content missed and **D)** the total number of off-targets for interrogation are shown for each individual replicate (all nominated sites) compared to the total # of high priority sites (Tier 1 to Tier 3) nominated as a biological triplicate. Specificity score was calculated as the cumulative frequency of UMI-corrected nomination events off-target divided by the number cumulatively between the on-target and off-targets.

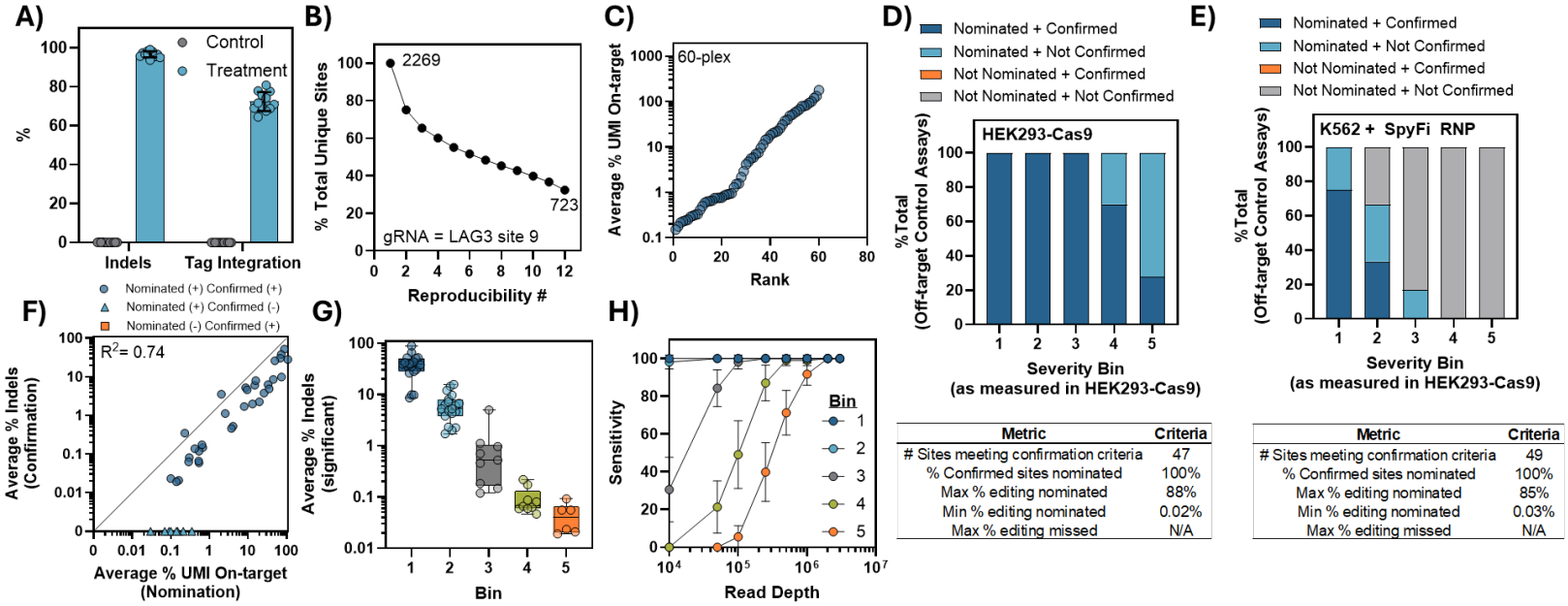

Metric	Criteria
# Sites meeting confirmation criteria	47
% Confirmed sites nominated	100%
Max % editing nominated	88%
Min % editing nominated	0.02%
Max % editing missed	N/A

Metric	Criteria
# Sites meeting confirmation criteria	49
% Confirmed sites nominated	100%
Max % editing nominated	85%
Min % editing nominated	0.03%
Max % editing missed	N/A

Figure 4. Quality control procedures for confirming assay sensitivity and read requirements. To create a positive control for UNCOVERseq process quality control, we extensively characterized a promiscuous *LAG3* (site 9) gRNA in HEK293-Cas9 using 12 biological replicate transfections with paired controls (no gRNA). Following transfection, **A**) indel frequency and tag integration frequencies were measured at the *LAG3* on-target site via NGS and **B)** the frequency of unique sites relative to the cumulative total reaching each reproducibility frequency is shown. **C)** Twelve sites were selected per frequency bin (Severity Bin 5 = <0.49%; Severity Bin 4 = 0.50% – 0.99%; Severity Bin 3 = 1 - 9.9%; Severity Bin 2 = 10 - 49.9%; Severity Bin 1 = >50% UMI reads relative to the on-target) for routine targeted sequencing with average nomination frequency shown. To test application of this, paired confirmation was performed in **D)** a highly promiscuous condition (HEK293-Cas9; n = 3 biological replicates) and **E)** high-specificity condition (K562 nucleofected SpyFi RNP; n = 3 biological replicates) and the status of each of the 60 measured sites meeting coverage criteria (>1,000x) recorded. **F)** Quantification of HEK293-Cas9 confirmation and nomination frequencies is plotted with final status shown as either Nominated and Confirmed (blue circle), Nominated and Not Confirmed (light blue triangle), or Not Nominated and Confirmed (orange square) with **G)** confirmed indel frequencies per bin shown. **H)** Downsampling of the HEK293-Cas9 *LAG3* nomination samples (n = 12 biological replicates) was performed and sensitivity per Severity Bin calculated for recovering all 60 *LAG3* positive control confirmation loci.

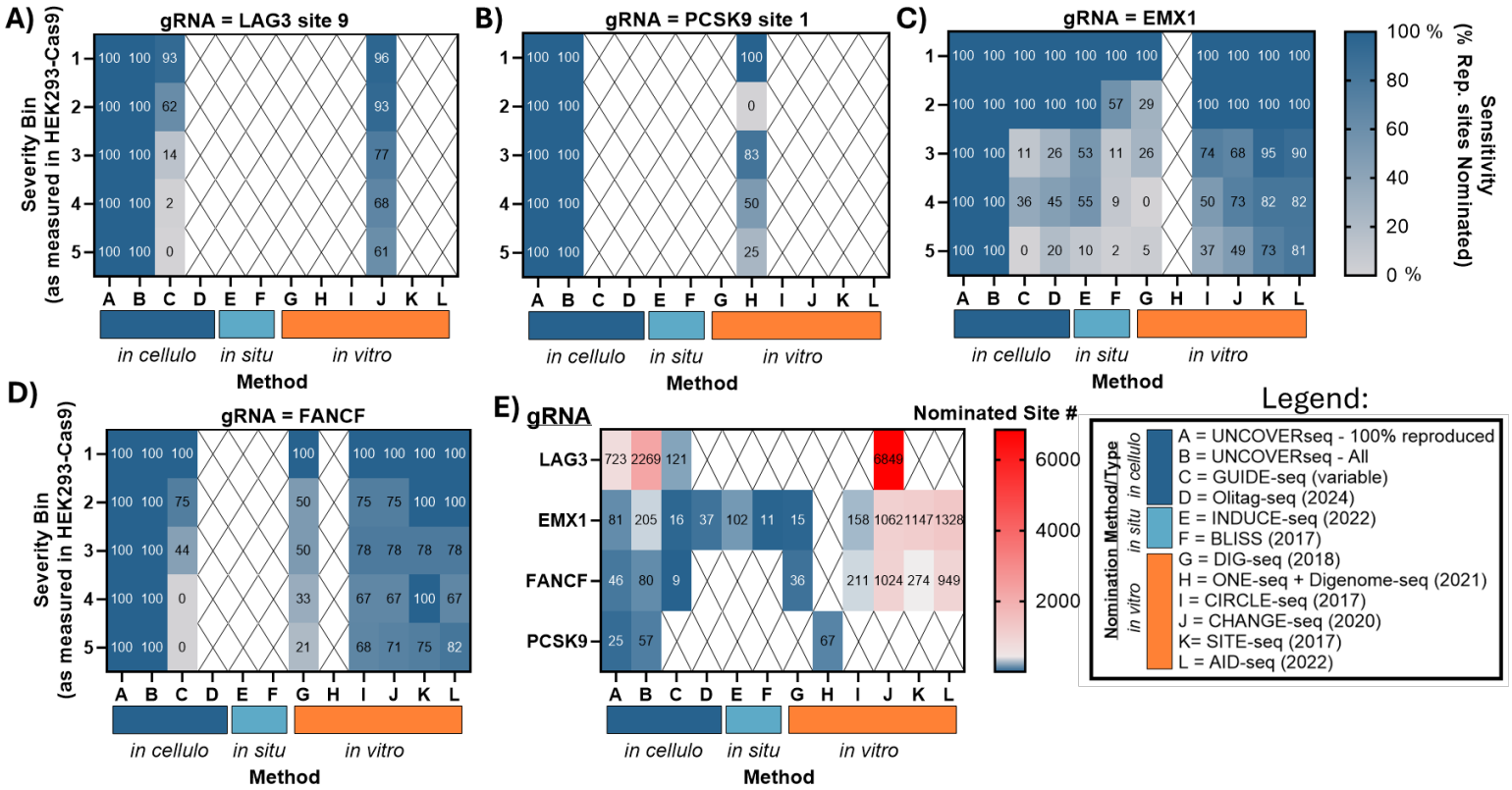

Figure 5. Comparative analysis of UNCOVERseq to other nomination technologies. Comparison of the sensitivity of other published accounts of nomination technologies to nominate 100% reproducible UNCOVERseq off-target sites using **A)** LAG3 site 9 (n = 12 nomination replicates) **B)** PCSK9 site 1 (n = 6 nomination replicates) **C)** EMX1 (n = 6 nomination replicates) and **D)** FANCF (n = 6 nomination replicates). **E)** Total number of off-targets nominated per nomination method per gRNA with color gradient shifts at the number of off-targets easily interrogated using amplicon sequencing (<250 targets; blue/grey) vs those more challenging to interrogate using amplicon sequencing (>250; grey/red). Legend displays the corresponding method to each column in the heatmaps along with the corresponding method type (*in cellulo, in situ, in vitro*). Rep. sites; Reproducible UNCOVERseq sites between all replicates. UNCOVERseq – All represents all Tier 1 to Tier 3 sites from the experiments.

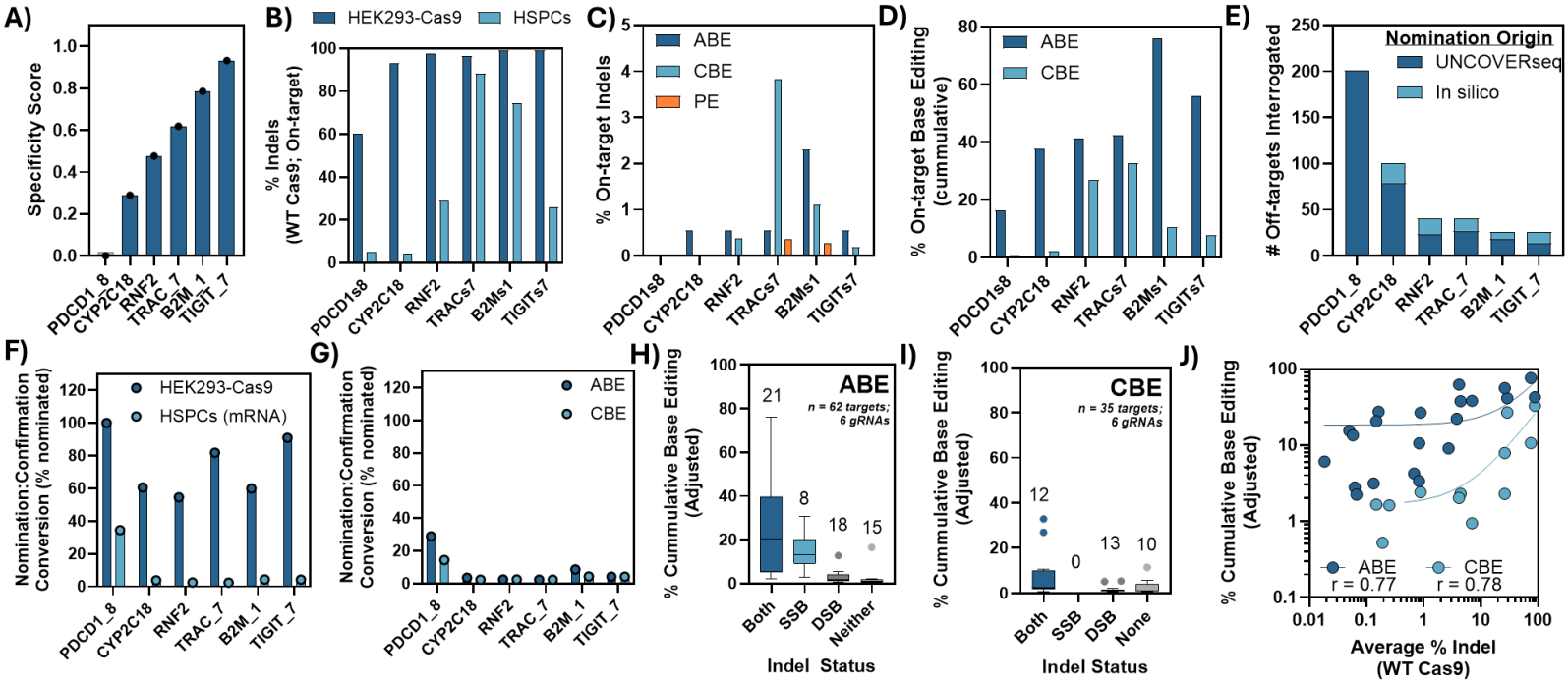

Figure 6. On-target and off-target editing in HEK293-Cas9 and HSPCs. A) Six gRNAs with a single targeted ABE or CBE base were selected with specificity scores shown. HEK293-Cas9 (n = 1) and HSPCs (n = 3 donors), with simultaneous delivery of the corresponding HiFi Cas9 mRNA, were delivered each gRNA and had **B)** on-target indel editing quantified by NGS. HSPCs were also delivered mRNA with either the *S.p.* Cas9-ABE8 or *S.p.* Cas9-CBE fusion for each gRNA and had **C)** indel editing and **D)** base editing quantified using NGS. **E)** Multiplexed amplicon sequencing (rhAmpSeq) panels were created for each gRNA for off-target quantification based on origin from UNCOVERseq or *in silico* nomination (*in silico)* with the number of targets interrogated per gRNA shown. After sequencing/confirmation of off-targets in all conditions, the frequency that UNCOVERseq nominated sites converted to true positives was measured for **F)** *S. p.* Cas9 or HiFi Cas9 indel editing and **G)** *S. p.* Cas9 base editing conditions. Confirmed base editing sites were categorized by their respective indel confirmation status (DSB = wildtype *S.p. Cas9;* SSB = ABE/CBE nickase) with cumulative base editing plotted for **H)** ABE and **I)** CBE editing conditions. **J)** Frequencies were plotted for all confirmed ABE/CBE sites with both SSB and DSB confirmation with the respective DSB indel frequency and Spearman r calculated. Line indicates linear regression for ABE (dark blue) and CBE (light blue).

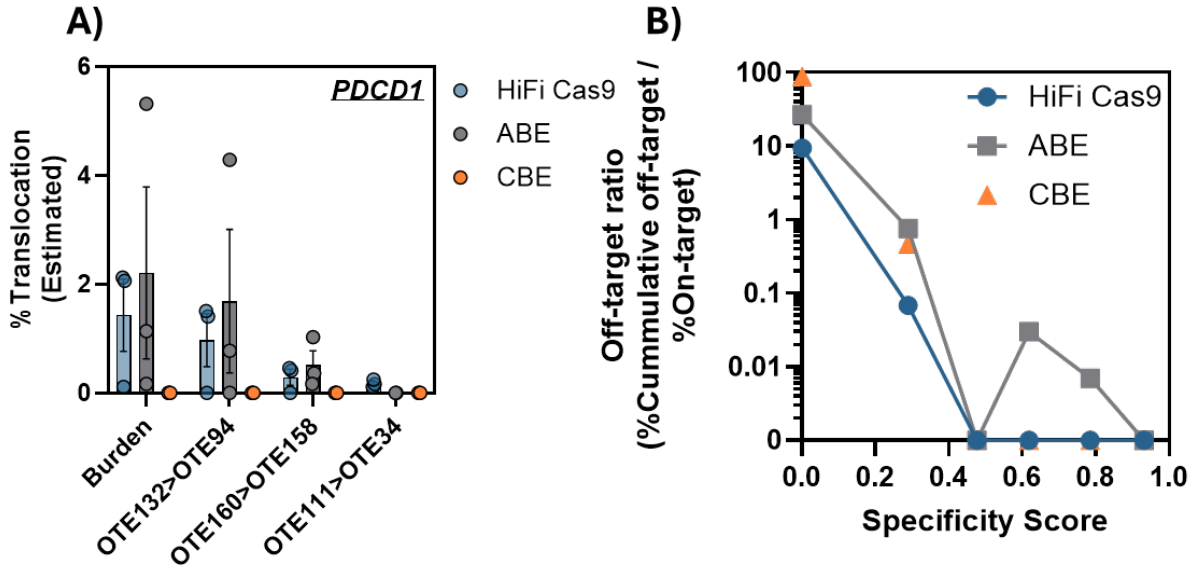

Figure 7. Translocation and cumulative off-target risk. Targeted sequencing data was used for translocation detection between on-target:off-target and off-target:off-target assays in the same pool. **A)** Translocation quantification (FDR < 0.01) at the *PDCD1* site 8 gRNA across different editor modalities in HSPCs and **B)** the cumulative off-target ratio (% cumulative off-target events / % on-target) were calculated for each gRNA in HSPCs with mRNA delivery. Cumulative off-target events for all modalities consider base editing, indel editing, and translocations.

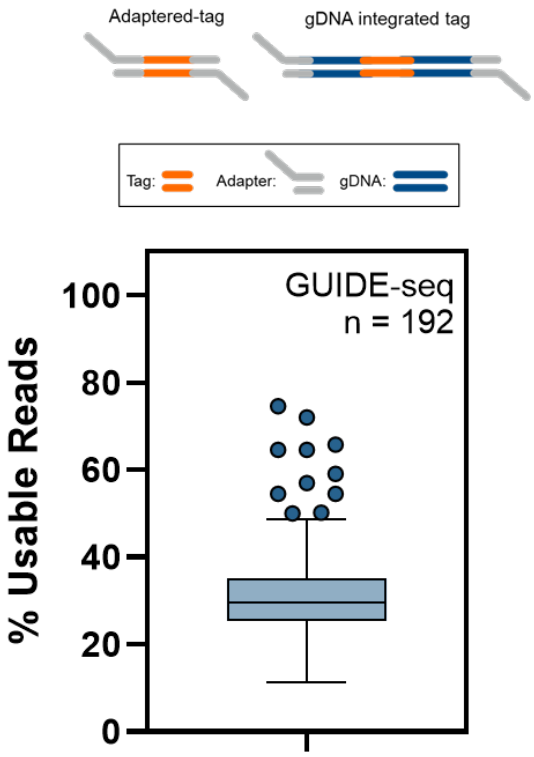

Supplementary Figure 1. Quantification of read loss due to adaptered tag in the GUIDE-seq protocol. A depiction is shown regarding what kind of events form during library preparation with GUIDE-seq, with the usable reads (non-dsDNA:adapter reads) measured across nominating off-targets for 192 gRNAs in K562 (n = 1 per gRNA)**.**

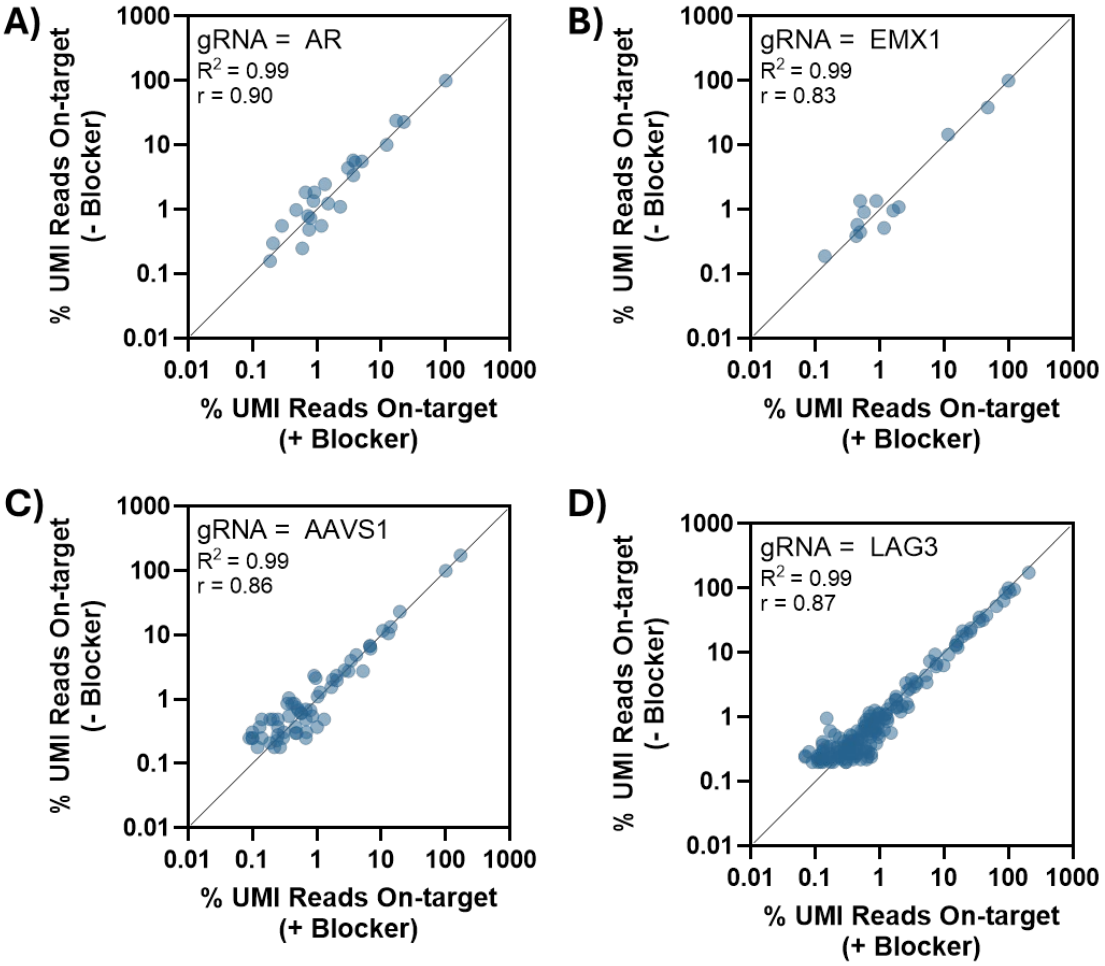

Supplementary Figure 2. Comparison of UNCOVERseq nomination frequencies with and without dsDNA tag:adapter blocker. Comparison of average nomination frequencies (normalized to the UMI-corrected on-target frequency) in K562 (n = 3 per gRNA) with and without the dsDNA tag:adapter blocker (Blocker) from shared sites for the following gRNAs: **A)** *AR*, **B)** *EMX1*, **C)** AAVS1, and **D)** *LAG3*.

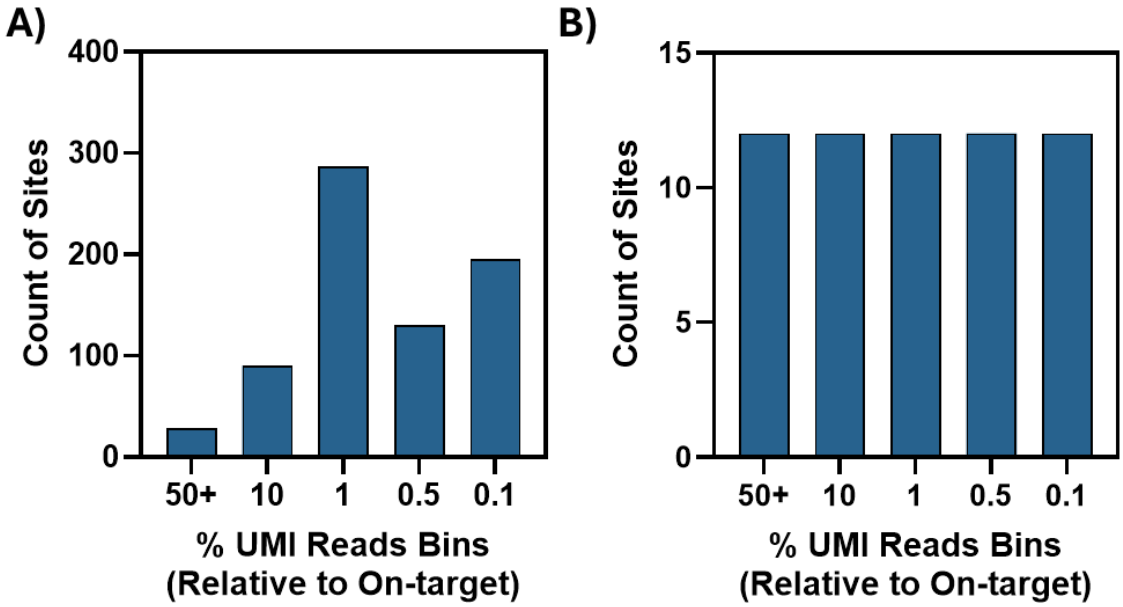

Supplementary Figure 3. Site selection for LAG3 process control panel. UNCOVERseq was used to nominate targets of the *LAG3* site 9 gRNA in HEK293-Cas9 (n = 12 biological replicates) and **A)** the average nomination frequency (normalized to the on-target frequency) of each site was binned into 5 frequency bins (0.10 – 0.49%; 0.50% – 0.99%; 1 - 9.9%; 10 - 49.9%; >50% UMI reads relative to the on-target). **B)** Selected sites per frequency bin for interrogation as a part of process control 60-plex.

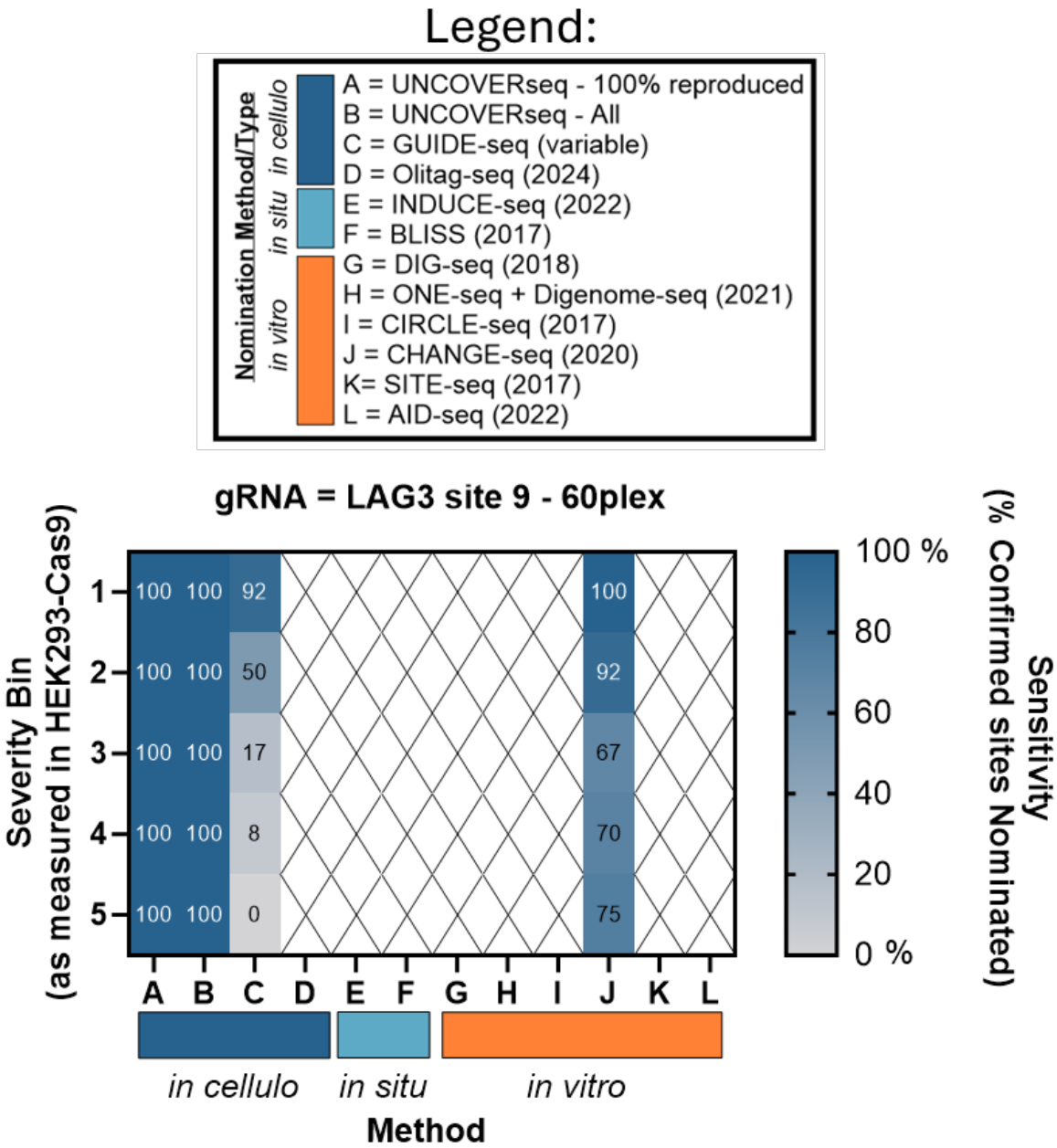

Supplementary Figure 4. Comparative analysis of UNCOVERseq at the confirmed LAG3 60-plex site list to other nomination technologies. Comparison of the sensitivity of other published accounts of nomination technologies to nominate sites previously confirmed UNCOVERseq off-target sites at the *LAG3* site 9 (n = 12 nomination replicates) gRNA.

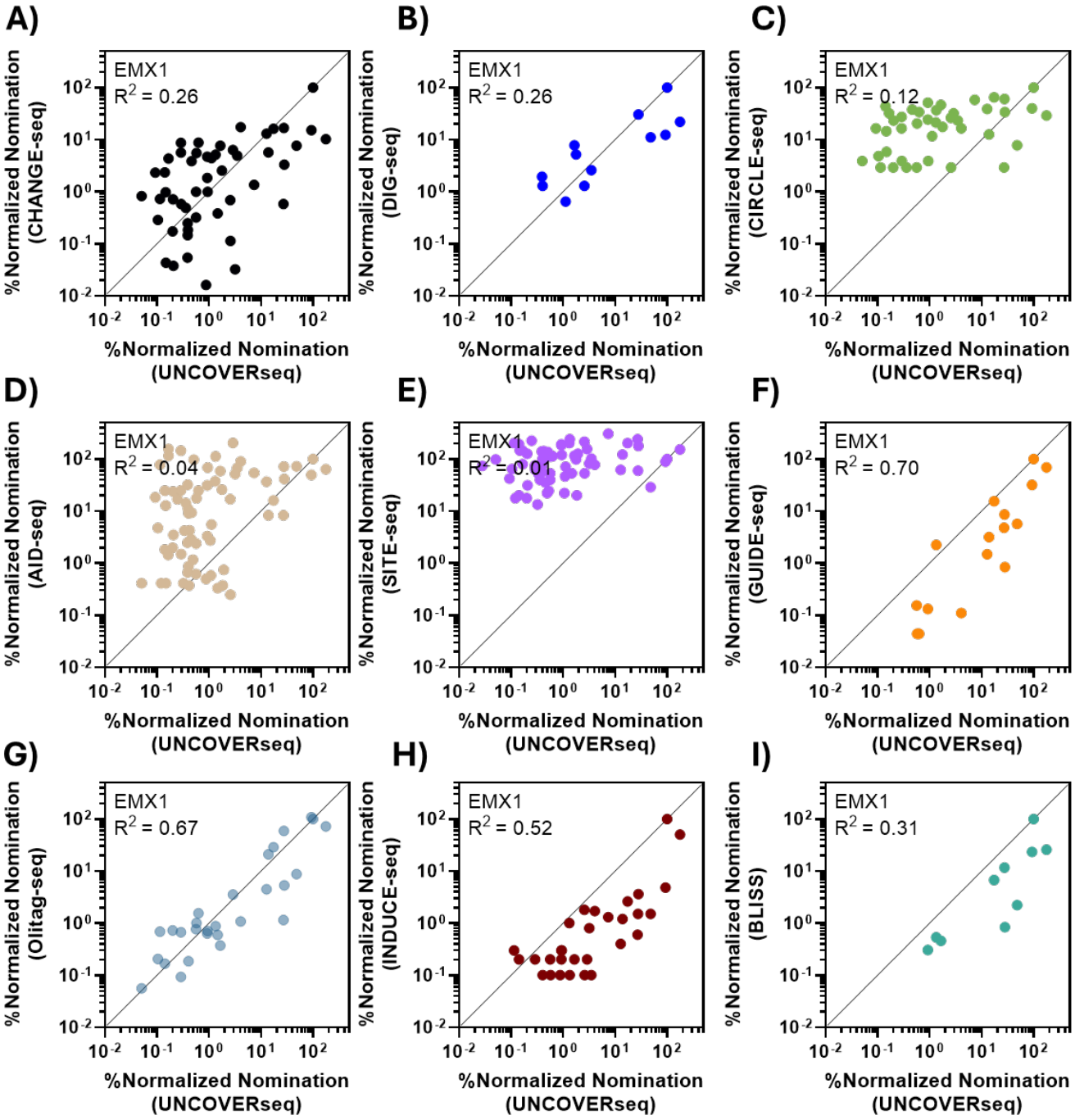

Supplementary Figure 5. Comparative analysis of UNCOVERseq nomination frequencies to other previously published technologies at the EMX1 site. Comparison of the nomination frequencies from shared sites of published accounts of nomination technologies (normalized to the on-target frequency) to average nomination frequency of fully reproduced EMX1 UNCOVERseq nomination (n = 6 replicates). Biochemical *in vitro* methods displayed are **A)** CHANGE-seq **B)** DIG-seq **C)** CIRCLE-seq **D)** AID-seq and **E)** SITE-seq. Cell-based *in cellulo* or *in situ* methods displayed are **F)** GUIDE-seq **G)** Olitag-seq **H)** INDUCE-seq and **I)** BLISS

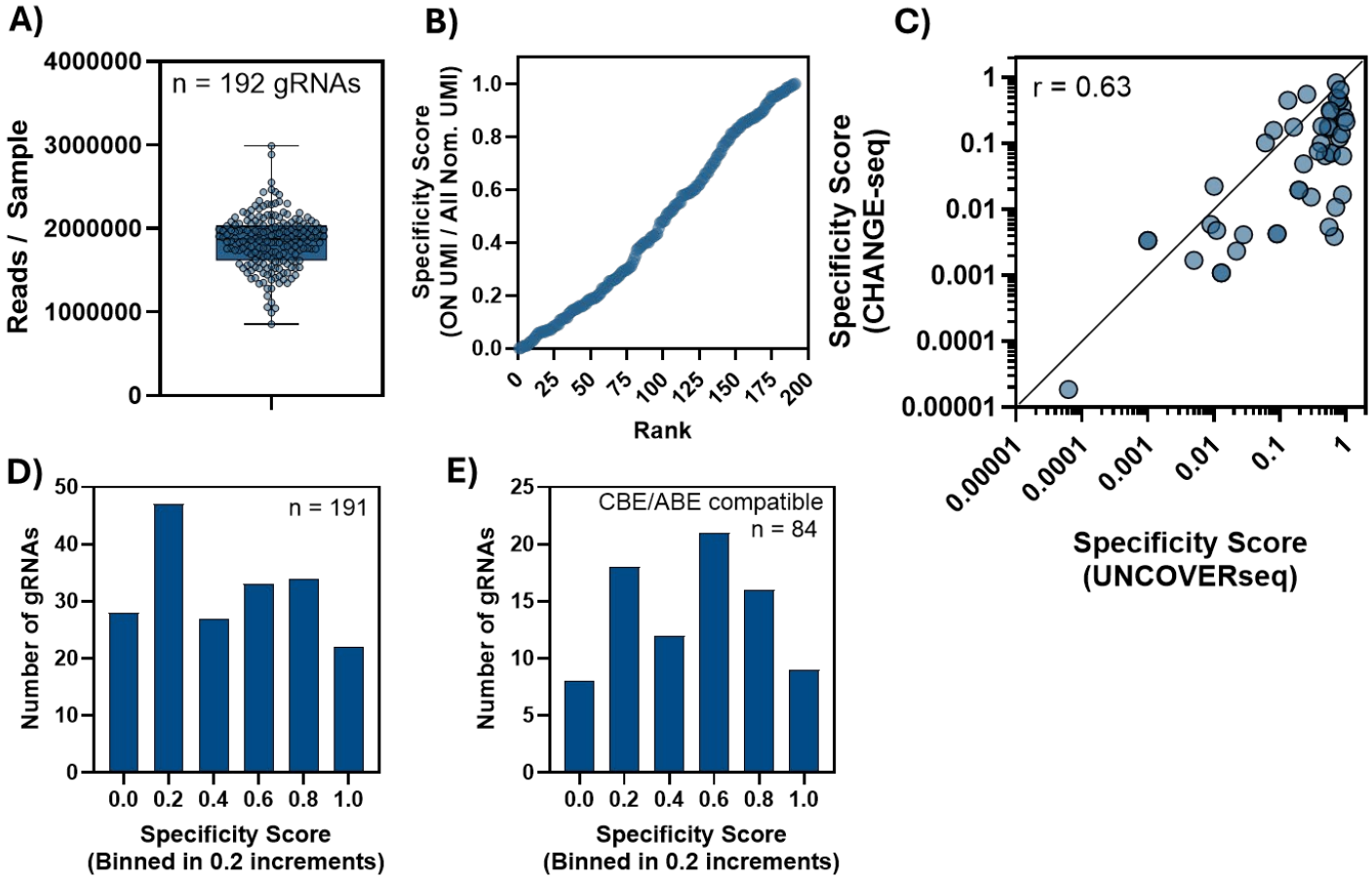

Supplementary Figure 6. UNCOVERseq gRNA specificity scores for nominated gRNAs and ABE/CBE-compatible gRNAs. 192 gRNAs were individually transfected into HEK293-Cas9 to perform UNCOVERseq. **A)** Read depth per sample of each gRNA and **B)** the rank-order specificity score were quantified. **C)** Comparison of derived specificity scores to those from the published CHANGE-seq method (2020). Specificity scores were binned from 0 to 1 in 0.2 increments and the # of gRNAs per binned counted for **D)** all gRNAs and **E)** gRNAs that met ABE criteria (at least one "A" in 5' position 4 – 7) and CBE criteria (at least one "C" in 5' position 4 – 8).

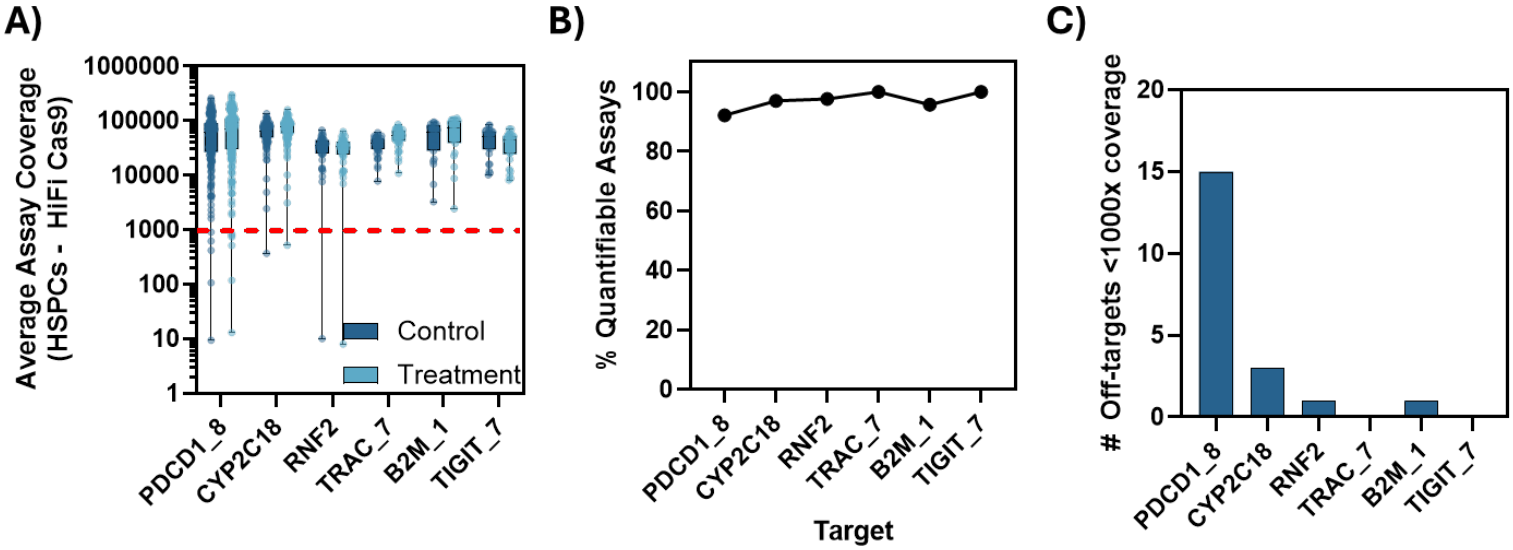

Supplementary Figure 7. Sequencing performance per gRNA off-target panel. A) Average targeted sequencing coverage for each assay within the multiplexed rhAmpSeq panel created for confirmation of off-targets is plotted using paired treatment/controls for the HSPC HiFi Cas9 editing condition (n = 3 per treatment) with the >1,000x coverage requirement depicted (dotted red line). **B)** Frequency of all replicates reaching >1,000x for each target in the panel and **C)** the number of targets failing to meet this threshold is quantified per gRNA.

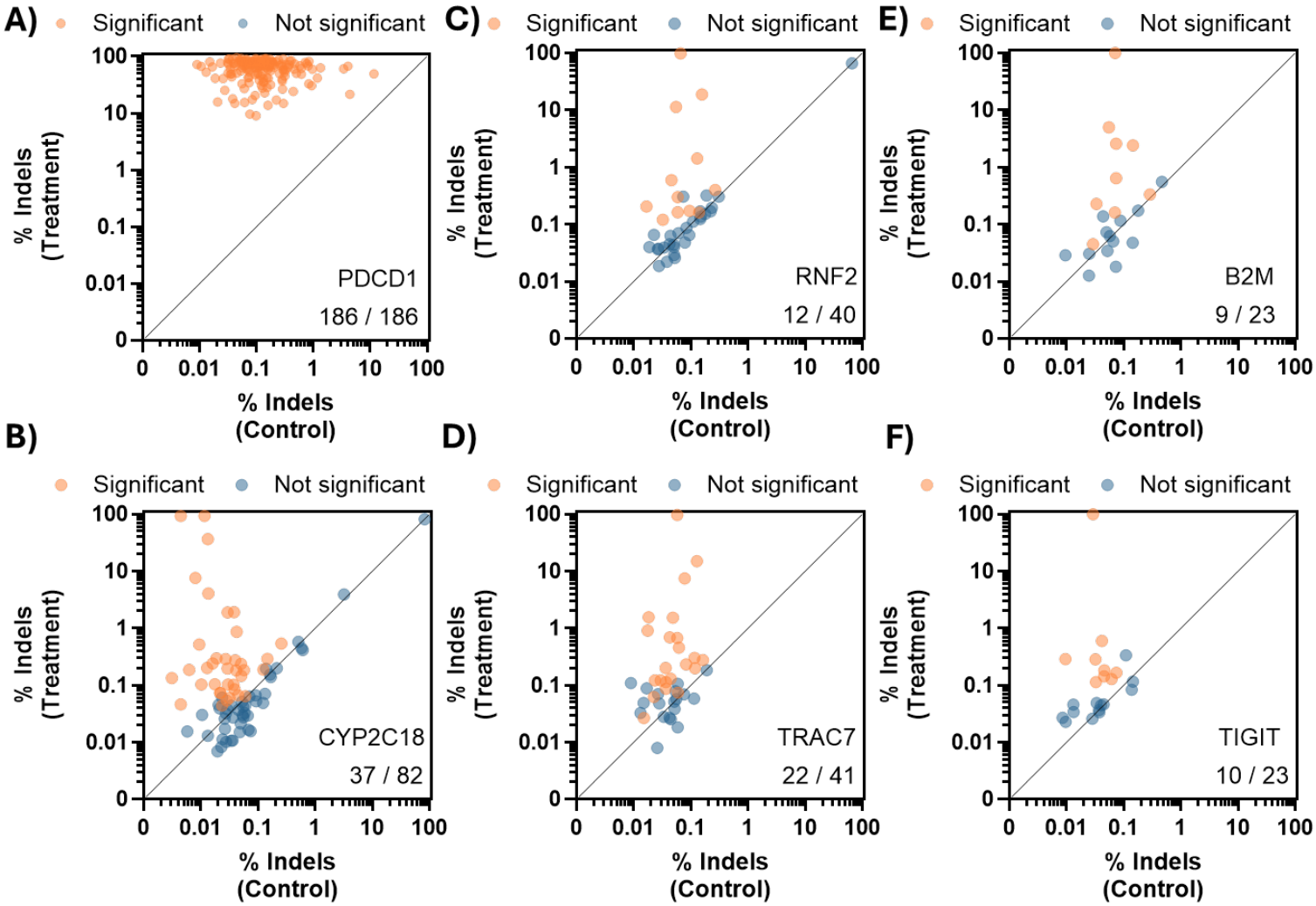

Supplementary Figure 8. Confirmation in HEK293–Cas9 (indels). Editing quantification at assays with >1,000x coverage. Each dot represents a gRNA on/off-target with the average raw frequency of indels of the control (x-axis) and treatment (y-axis) plotted. Blue dots indicate sites with no statistical significance while orange dots indicate significant sites (p adj<0.05) for the **A)** *PDCD1* site 8, **B)** *CYP2C18*, **C)** *RNF2*, **D)** T*RAC* site 7, **E)** *B2M* site 1, and **F)** *TIGIT* site 7 gRNAs. Text at the bottom right displays the total number of confirmed sites out of all interrogated with sufficient depth (>1,000x).

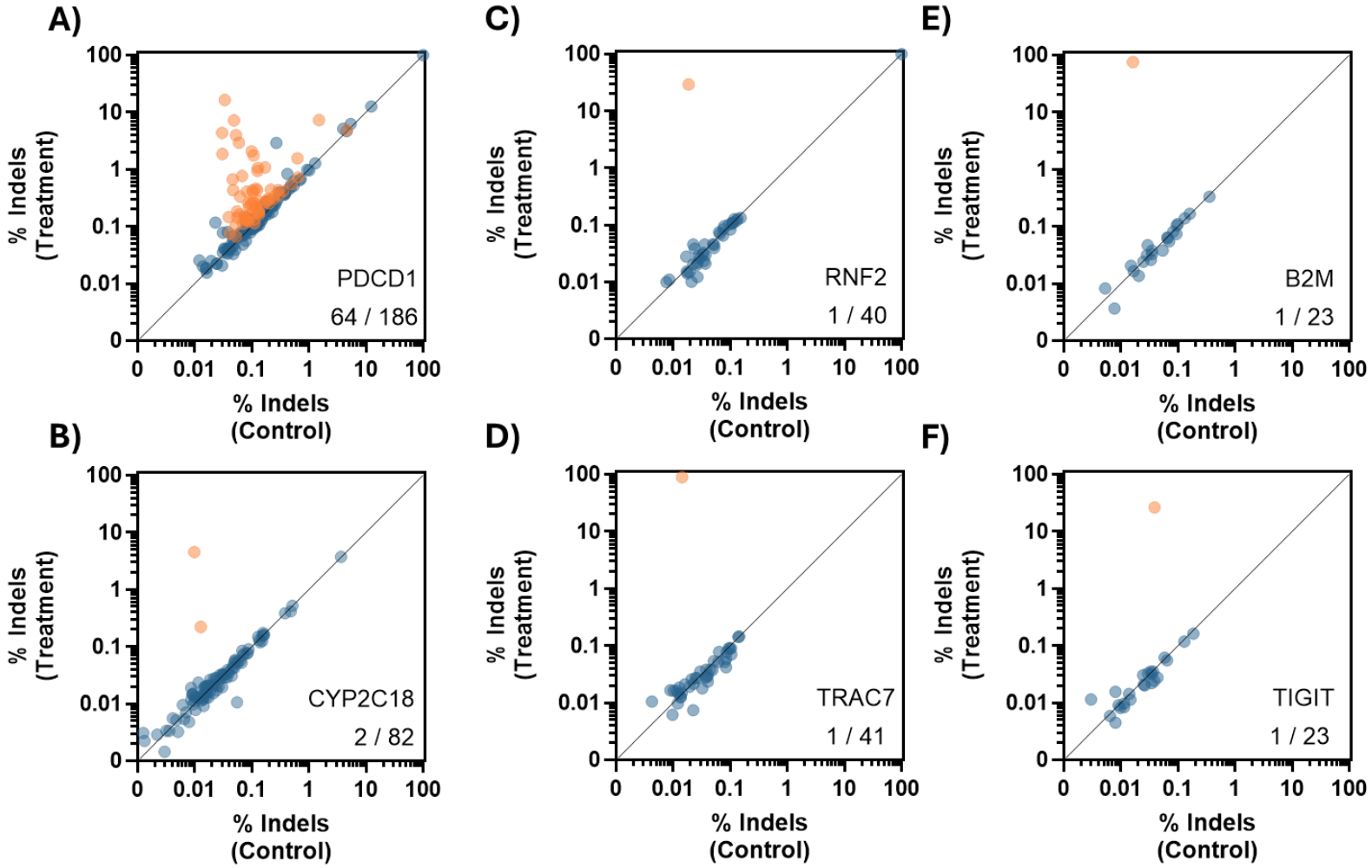

Supplementary Figure 9. Confirmation in HSPCs with HiFi Cas9 delivered as mRNA (indels). Editing quantification at assays with >1,000x coverage. Each dot represents a gRNA on/off-target with the average raw frequency of indels of the control (x-axis) and treatment (y-axis) plotted. Blue dots indicate sites with no statistical significance while orange dots indicate significant sites (p adj<0.05) for the **A)** *PDCD1* site 8, **B)** *CYP2C18*, **C)** *RNF2*, **D)** T*RAC* site 7, **E)** *B2M* site 1, and **F)** *TIGIT* site 7 gRNAs. Text at the bottom right displays the total number of confirmed sites out of all interrogated with sufficient depth (>1,000x).

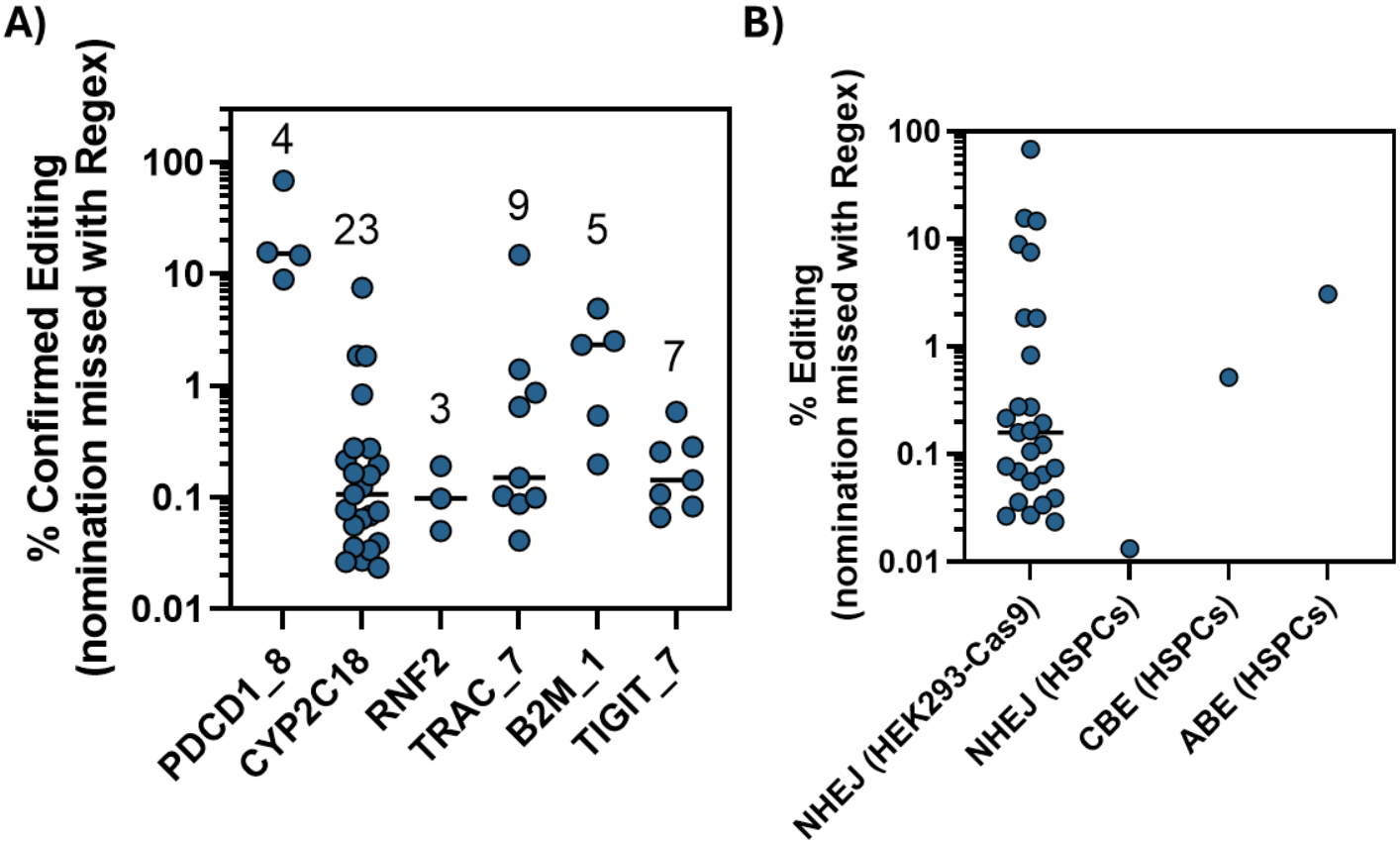

Supplementary Figure 10. Confirmable editing sites that can be missed with Regex alignment approach. Confirmed off-targets (p-value < 0.05) were intersected with those missed using the Regex method for determining off-target alignment distance < 7 and frequencies of these sites determined **A)** per gRNA in HEK293-Cas9 and **B)** per condition, between HEK293-Cas9 and HSPCs (HiFi Cas9, CBE, and ABE).

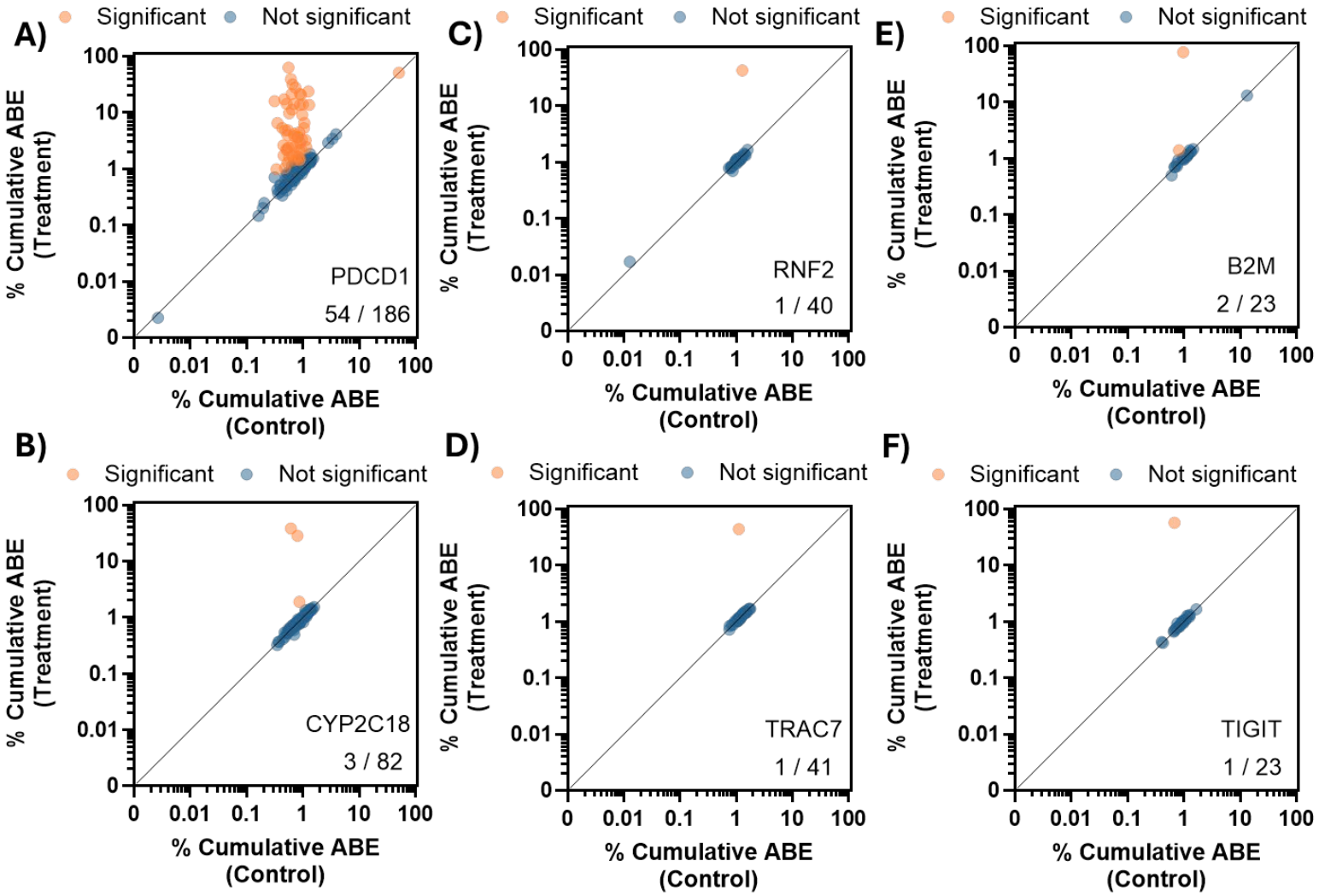

Supplementary Figure 11. Confirmation in HSPCs with wildtype *S.p.* Cas9-ABE delivered as mRNA (ABE). Editing quantification at assays with >1,000x coverage. Each dot represents a gRNA on/off-target with the average raw frequency of cumulative ABE transition events of the control (x-axis) and treatment (y-axis) plotted. Blue dots indicate sites with no statistical significance while orange dots indicate significant sites (p adj<0.05) for the **A)** *PDCD1* site 8, **B)** *CYP2C18*, **C)** *RNF2*, **D)** T*RAC* site 7, **E)** *B2M* site 1, and **F)** *TIGIT* site 7 gRNAs. Text at the bottom right displays the total number of confirmed sites out of all interrogated with sufficient depth (>1,000x).

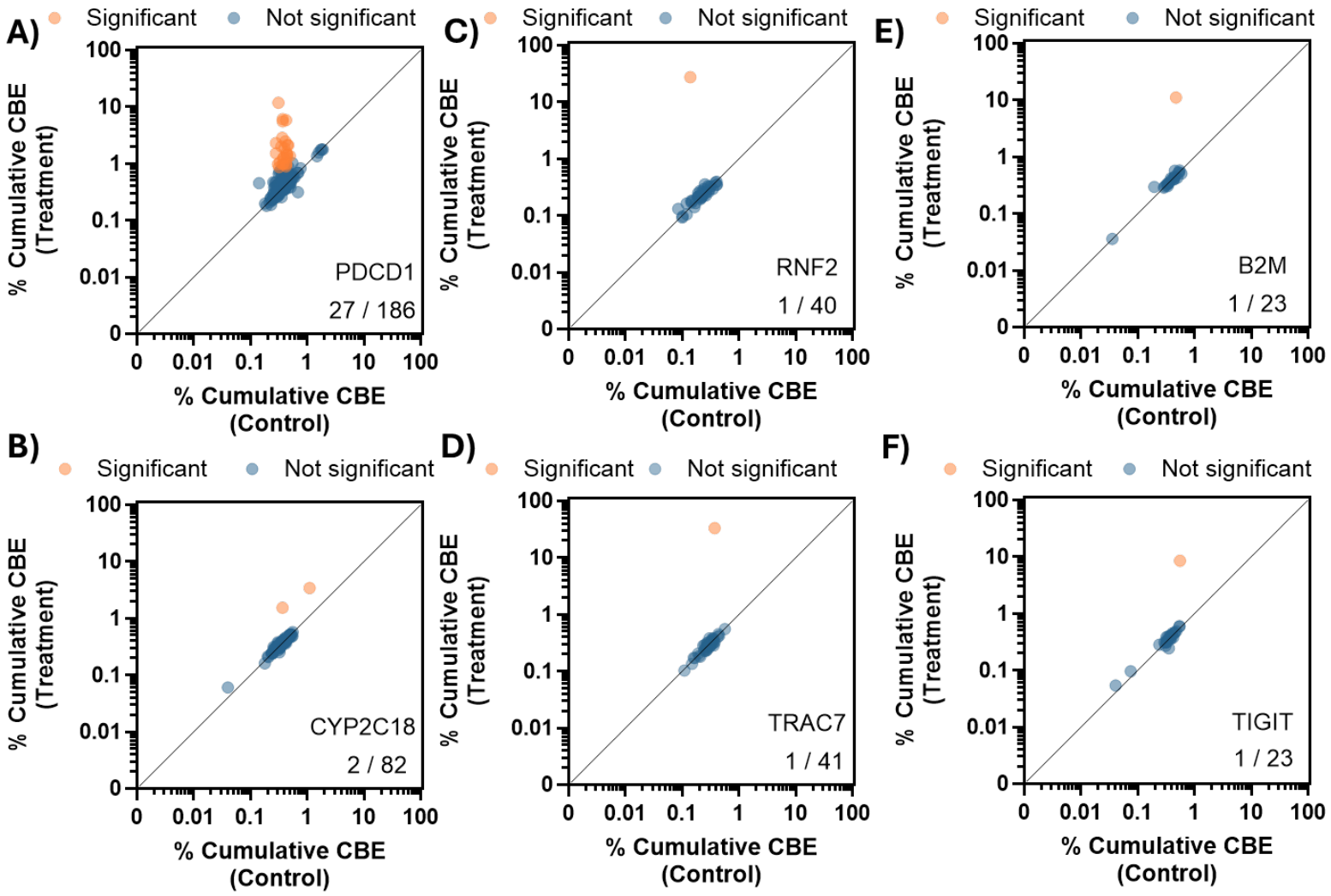

Supplementary Figure 12. Confirmation in HSPCs with wildtype *S.p.* Cas9-CBE delivered as mRNA (CBE). Editing quantification at assays with >1,000x coverage. Each dot represents a gRNA on/off-target with the average raw frequency of cumulative CBE transition events of the control (x-axis) and treatment (y-axis) plotted. Blue dots indicate sites with no statistical significance while orange dots indicate significant sites (p adj<0.05) for the **A)** *PDCD1* site 8, **B)** *CYP2C18*, **C)** *RNF2*, **D)** T*RAC* site 7, **E)** *B2M* site 1, and **F)** *TIGIT* site 7 gRNAs. Text at the bottom right displays the total number of confirmed sites out of all interrogated with sufficient depth (>1,000x).

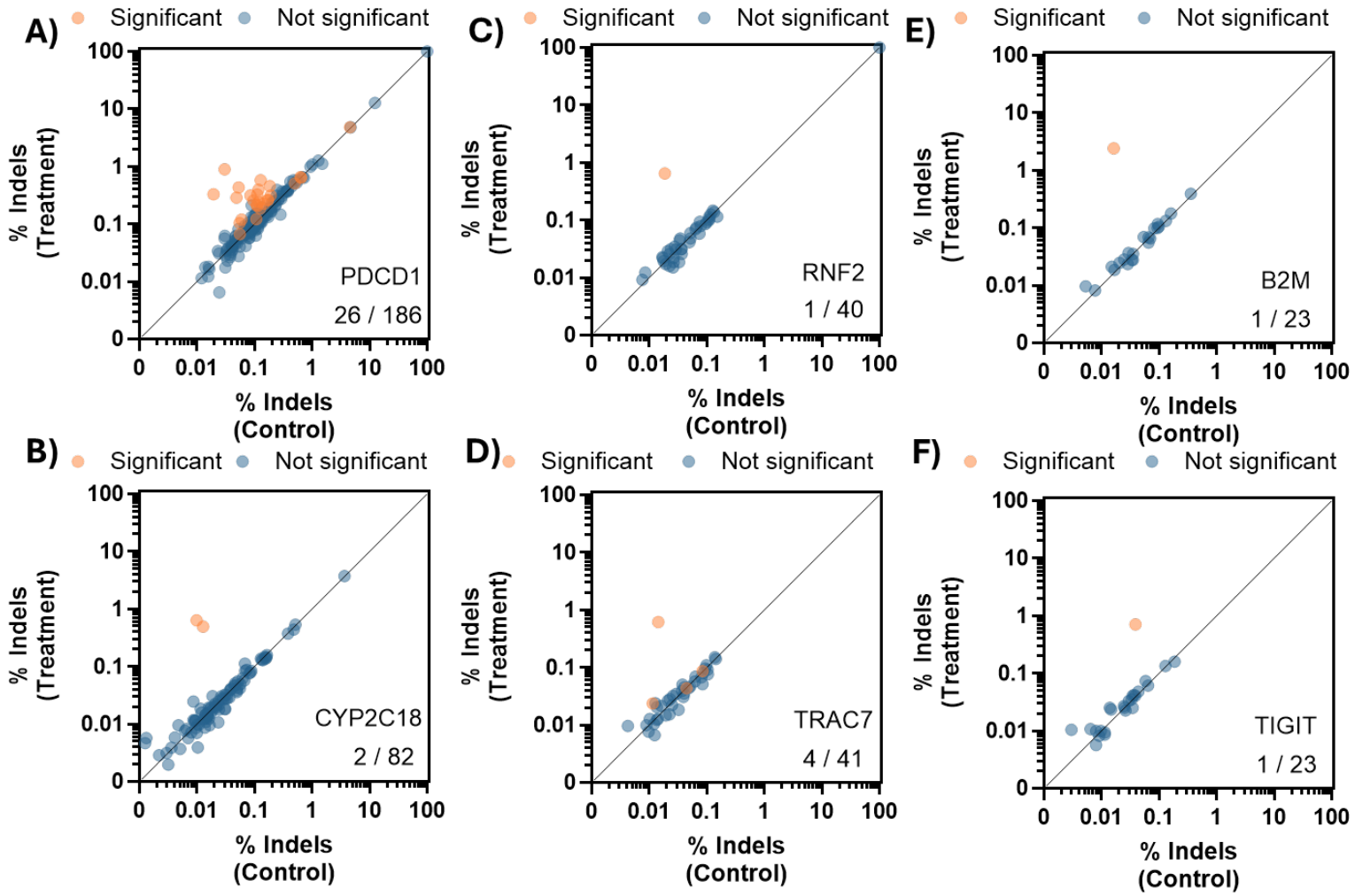

Supplementary Figure 13. Confirmation in HSPCs with wildtype *S.p.* Cas9-ABE delivered as mRNA (indels). Editing quantification at assays with >1,000x coverage. Each dot represents a gRNA on/off-target with the average raw frequency of indel events of the control (x-axis) and treatment (y-axis) plotted. Blue dots indicate sites with no statistical significance while orange dots indicate significant sites (p adj<0.05) for the **A)** *PDCD1* site 8, **B)** *CYP2C18*, **C)** *RNF2*, **D)** T*RAC* site 7, **E)** *B2M* site 1, and **F)** *TIGIT* site 7 gRNAs. Text at the bottom right displays the total number of confirmed sites out of all interrogated with sufficient depth (>1,000x).

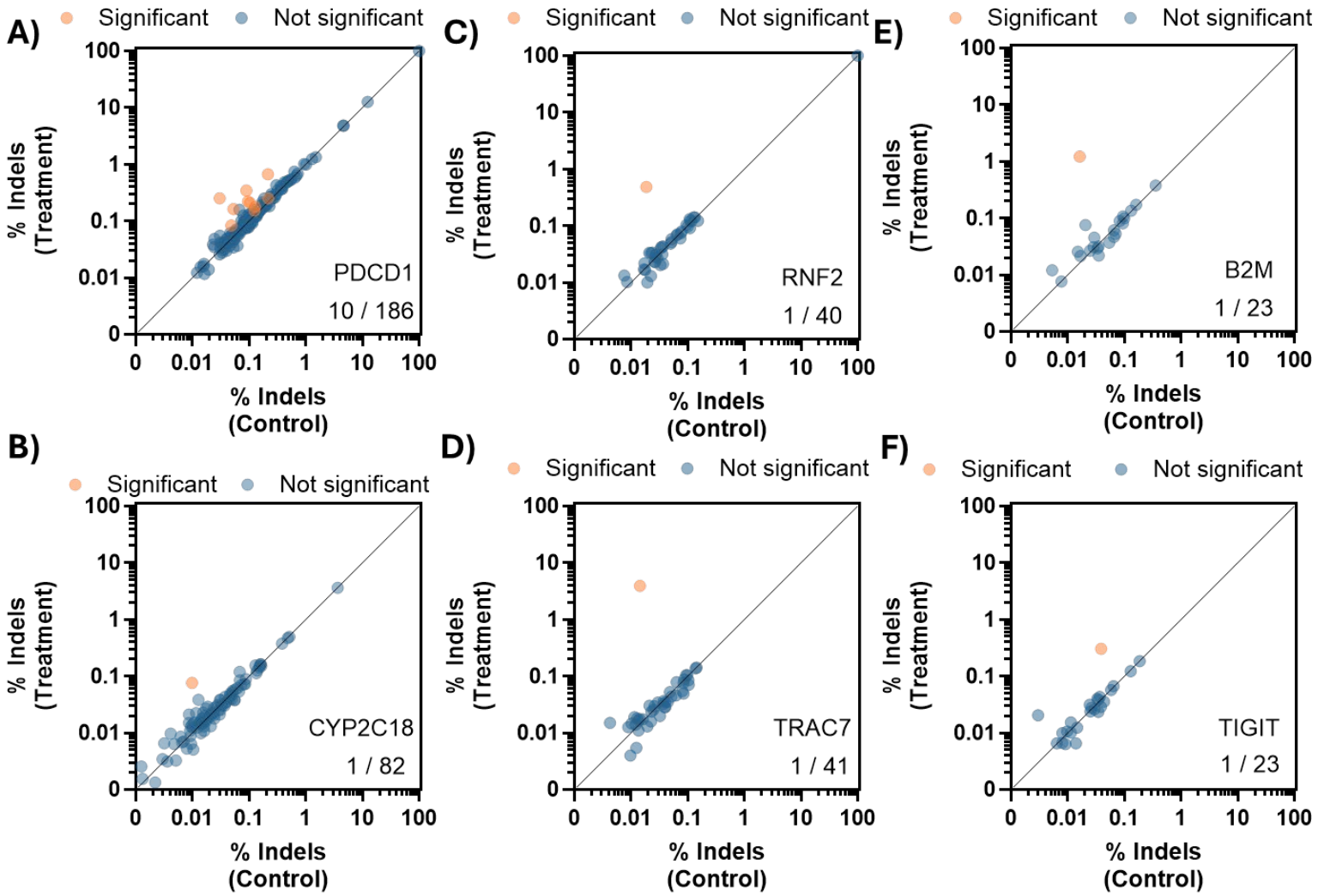

Supplementary Figure 14. Confirmation in HSPCs with wildtype *S.p.* Cas9-CBE delivered as mRNA (indels). Editing quantification at assays with >1,000x coverage. Each dot represents a gRNA on/off-target with the average raw frequency of indels of the control (x-axis) and treatment (y-axis) plotted. Blue dots indicate sites with no statistical significance while orange dots indicate significant sites (p adj<0.05) for the **A)** *PDCD1* site 8, **B)** *CYP2C18*, **C)** *RNF2*, **D)** T*RAC* site 7, **E)** *B2M* site 1, and **F)** *TIGIT* site 7 gRNAs. Text at the bottom right displays the total number of confirmed sites out of all interrogated with sufficient depth (>1,000x).

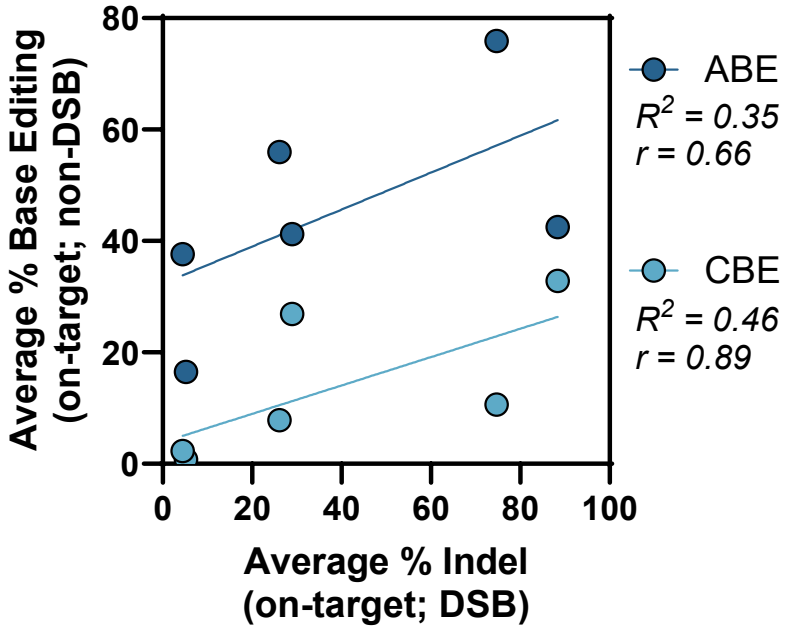

Supplementary Figure 15. On-target indel and base editing correlations in HSPCs. Frequencies were plotted for all on-target ABE/CBE sites with both SSB and DSB along with the respective DSB indel frequency (wildtype Cas9) and Spearman r calculated.